Bulk Dynamics from Holographic Tensor Networks

Conor Crump, 8165335

First Examiner: Wilke van der Schee
Second Examiner: Umut Gürsoy

A thesis presented for the degree of
Master of Science

Theoretical Physics
Utecht University
December 2023

Dedicated to my grandfather
Proinsias Brinkley (1943 - 2022)

Contents

1 Introduction

The failure of standard quantization techniques when applied to the Einstein field equations, characterized by the need for an infinite number of counterterms, has led many to believe that, despite their success in describing large-scale gravity, the Einstein field equations are in fact an effective field theory [1] of an, as yet undiscovered, UV complete theory of quantum gravity.

Today one of the best clues we have about the nature of quantum gravity is the holographic principle [2, 3]. Inspired by the discovery that the entropy of a black hole is proportional to its area [4], the principle proposes that for a quantum gravitational system with d spacetime dimensions, the system is completely defined by a non-gravitational quantum field theory on a $d-1$ dimensional spacetime. While the principle is just a conjecture, it was put on much stronger ground when it was shown that certain string theories are dual to conformal field theories with one less spatial dimension [5]. This duality is today known as the AdS/CFT correspondence. While AdS/CFT was borne out of string theory, today it very much has a life of its own, making far-reaching impacts in various fields well outside the scope of quantum gravity, such as condensed matter [6], QCD [7] and quantum information theory [8].

The connection with quantum information theory has been particularly impactful, as it is now believed that information-theoretic ideas are essential to understanding quantum gravity. This connection started with a generalization of Bekenstein's black hole entropy formula to the AdS/CFT context [9] which led to the realization that the entanglement present in the CFT gives rise to the emergent spacetime geometry. Shortly thereafter a connection between quantum error correcting codes and the manner in which the gravitational information is encoded in the CFT degrees of freedom was put forward [10]. The connection

with entanglement has subsequently allowed for the construction of various toy models of the correspondence based on tensor networks [11, 12].

Tensor networks are a tool originally used by the condensed matter community to build efficient approximations for the quantum states of many body systems [13]. The way this efficiency is achieved is by designing the network geometry such that it targets quantum states that have the same entanglement structure as the state being approximated. It was first realized in [11] that this geometrization of entanglement is conceptually similar to AdS/CFT and in particular the multiscale entanglement renormalization ansatz (MERA) [14] class of tensor networks exhibit some properties that are tantalizingly similar to the AdS/CFT correspondence. Since then various new tensor network toy models have been produced and refined [12, 15, 16, 17], and new, tensor network inspired, conjectures about holography extending even beyond AdS/CFT have been put forward [18, 19].

However, despite the success of tensor network models for holography, a satisfactory understanding of how to model the dynamics of the emergent spacetime has yet to develope. Some prior attempts at tackling this issue do exist [20, 21, 22], however they each have their limitations, and in particular none of them allow for the possible simulation of bulk dynamics on a computer.

The goal of this thesis then, is to introduce a new way in which tensors networks can be used to model holography such that that the emergent bulk geomtery can be dynamically evolved. This manner in which this is achieved is such that it is feasible to simulate the bulk for a reasonable system size.

The outline of the thesis is as follows. In section 2 we will give an overview of some essential ideas from quantum information theory that will appear throught the subsequent sections. In section 3 we will introduce the AdS/CFT correspondence and outline the different versions of the extremal surface methods for computing entanglement entropy. In section 4 we will review tensor networks with particular focus given to MERA as this will be the network type we ultimately use to build our model. In section 5 we introduce the original connection between MERA and holography as well as the HaPPY holographic codes. We will discuss the feasibility of using each of these networks to model dynamics. In section 6 we then explore two possible methods for modelling bulk dynamics with tensor networks. The first, requiring more work to be fully realized and finally, a version of MERA for which it is feasible that the dynamics of the emergent spacetime can be simulated.

Throughout this thesis we will work in units for which $c = \hbar = k_B = 1$.

2 Quantum Information Theory

Quantum information theory is, in essence, the study of noisy quantum systems or the theory of communication of qubits over noisy channels. As such, the objects of interest are not vectors in a Hilbert space, but probabilistic ensembles of quantum states. Given a set of n states $\{|\psi_1\rangle, |\psi_2\rangle, \ldots, |\psi_n\rangle\}$ and a probability distribution over these states $\{p_1, p_2, \ldots, p_n\}$, we can construct a *density matrix*

given by,

$$\rho = \sum_{i=1}^{n} p_i \left|\psi_i\right\rangle \left\langle\psi_i\right| . \tag{1}$$

As a consequence, we have promoted quantum states from elements of the Hilbert space $\mathcal{H}$ to elements of the space of linear operators acting on the Hilbert space, $L(\mathcal{H})$. By construction density matrices are positive semi-definite, Hermitian matrices with trace one. Density matrices allow us to accommodate both quantum and classical uncertainties in a single representation. As an added bonus the global phase redundancy of the state vector representation is no longer present, as the global phase factors from the bras and kets always cancel. It is important to note that many different choices of ensemble and distribution can correspond to the same density matrix and so the choice is not unique. However in the case of non-degenerate eigenvalues a density matrix does have a unique spectral decomposition, where the set of states are now an orthonormal set containing the eigenvectors of ρ and the probabilities are the eigenvalues.
The case most familiar from standard quantum mechanics, where there is no classical uncertainty, is colloquially referred to as a *pure state*. In this case, the density matrix is given by a rank one projection, $\rho = \left|\psi\right\rangle \left\langle\psi\right|$. All other density matrices of rank greater than one are referred to as *mixed states*.

We would, of course, like to be able to perform measurements on our quantum system. In the density matrix formalism, this is done by computing the trace of operators. Given an observable $\mathcal{A}$ and a density matrix ρ, the expectation value of $\mathcal{A}$ is given by,

$$\left\langle \mathcal{A} \right\rangle_{\rho} = \mathrm{Tr}\left[\mathcal{A}\rho\right] . \tag{2}$$

Similarly, a POVM measurement (positive operator valued measure) is a function $\mu(x)$ from a set of measurement outcomes Ω to the positive semi-definite matrices acting on $\mathcal{H}$, such that $\sum_{x\in\Omega} \mu(x) = I$. We then have that, given ρ,

$$\Pr(x) = \mathrm{Tr}[\mu(x)\rho]. \tag{3}$$

This is simply a restatement of Born's rule in the language of density matrices.

2.1 Multipartite Systems

We will often be interested in not just single quantum systems, but composite or multipartite systems. In such cases each subsystem will have its own Hilbert space and the Hilbert of the whole system is obtained by taking the tensor product of the subsystem Hilbert spaces. In other words, if our system is composed of N subsystems were the Hilbert space of subsystem i is denoted $\mathcal{H}_i$ then the full Hilbert space is,

$$\mathcal{H} = \mathcal{H}_1 \otimes \mathcal{H}_2 \otimes \cdots \otimes \mathcal{H}_N = \bigotimes_{i=1}^{N} \mathcal{H}_i. \tag{4}$$

Note that the elements of such a space are by definition tensors or order N. Quantum states are then given by,

$$|\psi\rangle = \sum_{i_1=1}^{d_1} \sum_{i_2=1}^{d_2} \cdots \sum_{i_N=1}^{d_N} T_{i_1 i_2 \cdots i_N} |i_1 i_2 \cdots i_N\rangle \,, \tag{5}$$

where d_i is the dimension of Hilbert space $\mathcal{H}_i$ and $|i_1 i_2 \cdots i_N\rangle$ is short hand for $|i_1\rangle \otimes |i_2\rangle \otimes \cdots \otimes |i_N\rangle$ with $\{|i_j\rangle\}$ being some basis for $\mathcal{H}_j$. Density matrices on such multipartite systems are again of the same form as Eq. (1), but with the bras and kets being elements of a tensor product Hilbert space as we have described.

2.1.1 The partial trace and reduced density matrices

Let's now suppose that for some multipartite quantum system, we only have access to a subsystem and the rest of the system, the environment, is a mystery to us. What information do we have access to? This question is answered by introducing a new operation called the *partial trace*. We can write the Hilbert space for our subsystem and environment as $\mathcal{H} = \mathcal{H}_S \otimes \mathcal{H}_E$, where both Hilbert spaces here may themselves be composed of multiple subsystems. Suppose we want to measure some observable on the subsystem of interest, $A_S \in L(\mathcal{H}_S)$. For some state on the entire system $\rho \in L(\mathcal{H})$, the expectation value is given by,

$$\langle A_S \rangle = \mathrm{Tr}\left[(A_S \otimes I_E)\rho\right]. \tag{6}$$

What we would like to know is whether there exists some density matrix for the subsystem, $\rho_S \in L(\mathcal{H}_S)$, such that,

$$\langle A_S \rangle = \mathrm{Tr}\left[(A_S)\rho_S\right], \tag{7}$$

for any observable or measurement A_S. We can answer this by expanding and equating (6) and (7).

$$\begin{aligned}
\mathrm{Tr}\left[(A_S)\rho_S\right] &= \mathrm{Tr}\left[(A_S \otimes I_E)\rho\right] \\
\sum_{i=1}^{d_S} \langle i|_S (A_S)\rho_S |i\rangle_S &= \sum_{i=1}^{d_S}\sum_{j=1}^{d_E} \langle i|_S \langle j|_E (A_S \otimes I_E)\rho |i\rangle_S |j\rangle_E \\
&= \sum_{i=1}^{d_S} \langle i|_S \left[\sum_{j=1}^{d_E} (I_S \otimes \langle j|_E)(A_S \otimes I_E)\rho(I_S \otimes |j\rangle_E)\right] |i\rangle_S \\
&= \sum_{i=1}^{d_S} \langle i|_S (A_S) \left[\sum_{j=1}^{d_E} (I_S \otimes \langle j|_E)\rho(I_S \otimes |j\rangle_E)\right] |i\rangle_S \,,
\end{aligned}$$

which leads us to,

$$\rho_S = \sum_{j=1}^{d_E} (I_S \otimes \langle j|_E)\rho(I_S \otimes |j\rangle_E) \equiv \mathrm{Tr}_E[\rho]. \tag{8}$$

The operation Tr_E is then the partial trace over $\mathcal{H}_E$. The resulting density matrix ρ_S is referred to as the *reduced density matrix* on $\mathcal{H}_S$ and encapsulates all the information we have access to by restricting to S.
Important to note is that the partial trace of a density matrix always produces a density matrix, i.e. a positive semidefinite matrix of trace one. Furthermore, the reduced density matrix of a pure state is far from guaranteed to be pure, and in fact, as we will see shortly its 'mixedness' will serve as an important measure of the entanglement between the system and the environment.

2.1.2 Purifications of quantum states

Flipping the script on this last statement about reduced density matrices we can ask if, given a mixed state, does there exist a pure state on a larger Hilbert space, such that its reduced density matrix is exactly our mixed state. This is indeed the case and such a pure state is referred to as a *purification*. Suppose our mixed state, $\rho \in L(\mathcal{H})$, has the following spectral decomposition,

$$\rho = \sum_{i=1}^{r} p_i \left|\psi_i\right\rangle \left\langle\psi_i\right|, \tag{9}$$

then any state of the following form is a purification of ρ,

$$\left|\Psi\right\rangle = \sum_{i}^{r} \sqrt{p_i} \left|\psi_i\right\rangle \otimes \left|e_i\right\rangle, \tag{10}$$

where $\{|e_i\rangle\}$ can be any orthonormal set that span a r dimensional subspace of any auxiliary Hilbert space $\mathcal{H}_E$, with $\dim \mathcal{H}_E \geq r$. Showing this is indeed a purification is straightforward,

$$\begin{aligned}
\mathrm{Tr}_E \left[\left|\Psi\right\rangle \left\langle\Psi\right|\right] &= \sum_{i}^{r} \sum_{j}^{r} \sqrt{p_i}\sqrt{p_j} \left|\psi_i\right\rangle \left\langle\psi_j\right| \mathrm{Tr}\left[\left|e_i\right\rangle \left\langle e_j\right|\right] \\
&= \sum_{i}^{r} \sum_{j}^{r} \sqrt{p_i}\sqrt{p_j} \left|\psi_i\right\rangle \left\langle\psi_j\right| \left\langle e_j | e_i\right\rangle \\
&= \sum_{i=1}^{r} p_i \left|\psi_i\right\rangle \left\langle\psi_i\right| \\
&= \rho
\end{aligned}$$

2.1.3 Schmidt decomposition

The form that we acquired through purification in Eq. (10) is in fact extremely convenient to work with in a much more general context. When dealing with bipartite pure states, if we can represent such a state in this form, we have immediate access to the eigenvalues (and so probability distributions) of both reduced matrices, as well as the eigenvectors of both. Thankfully it is always

possible to represent a bipartite state in this way, and this representation is known as the *Schmidt decomposition*.

Definition 1. *For any state, $|\psi\rangle \in \mathcal{H}_A \otimes \mathcal{H}_B$, there is always a representation, known as the Schmidt decomposition, of said state as follows,*

$$|\psi\rangle = \sum_{i=1}^{r} s_i \, |a_i\rangle \otimes |b_i\rangle \,,$$

where s_i are real positive numbers called the singular values or Schmidt coefficients, and where $\{|a_i\rangle\}$ and $\{|b_i\rangle\}$ are orthonormal sets in $\mathcal{H}_A$ and $\mathcal{H}_B$ respectively. Additionally, r is referred to as the Schmidt rank of $|\psi\rangle$.

It is easy to see from the definition that the reduced density matrices of $|\psi\rangle\langle\psi|$ are as follows,

$$\begin{aligned} \rho_A &= \sum_{i=1}^{r} s_i^2 \, |a_i\rangle\langle a_i| \\ \rho_B &= \sum_{i=1}^{r} s_i^2 \, |b_i\rangle\langle b_i| \,. \end{aligned} \tag{11}$$

This immediately tells us something important.

- The reduced density matrices of a bipartite pure state both have the same eigenvalues, namely the squares of the singular values of $|\psi\rangle$.

A further useful property of the Schmidt decomposition is that it is unique up to degeneracy of the singular values. This follows from the fact that the Schmidt decomposition is really just the *singular value decomposition* in disguise, which we will now show.

The key insight here is that $\mathcal{H}_A \otimes \mathcal{H}_B \cong \mathcal{H}_A \otimes \mathcal{H}_B^*$, which means every state in $\mathcal{H}_A \otimes \mathcal{H}_B$ can be represented by a $n \times m$ matrix $\mathbf{\Psi}$, where n and m are the dimesions of the two respective Hilbert spaces. With our bipartite state represented as a matrix, we can go to work applying the singular value decomposition,

$$\mathbf{\Psi} = USV^\dagger, \tag{12}$$

where U and V are unitary and S is diagonal with real positive entries. Denoting the columns of U and V as $|u_i\rangle$ and $|v_i\rangle$ respectively, and the diagonal entries of S as s_i, the equation can be rewritten as

$$\mathbf{\Psi} = \sum_{i=1}^{r} s_i \, |u_i\rangle\langle v_i| \,. \tag{13}$$

Written in this suggestive form it should be clear that the Schmidt and singular value decompositions are indeed equivalent.

2.2 Quantum Channels

Since we have expanded our definition of a quantum state from a vector in Hilbert space to a positive semidefinite operator acting on a Hilbert space, it should come as no surprise that we must also expand our definition for the types of transformations we can perform on our states. By the linearity of quantum mechanics, it is reasonable to expect that these transformations are linear. More specifically they are linear maps from linear operators to linear operators denoted by $L(L(\mathcal{H}))$. As these objects can be understood as operators acting on the space of operators, it is common to refer to them as *superoperators*. However, this definition is of course far too broad for our purposes. We specifically want superoperators that send quantum states to quantum states[1]. Superoperators that satisfy the necessary conditions are called *quantum channels* and are the most general form of transformation that can be performed on a quantum state, whether that be time evolution, measurement, quantum communication, or even renormalization [23].

So given a superoperator such as,

$$\Phi : L(\mathcal{H}_A) \to L(\mathcal{H}_B), \tag{14}$$

how can we ensure that it is a quantum channel? In fact, this can be done by imposing just two conditions.

Trace preserving: This first condition is quite self-explanatory. Since all quantum states must have normalized trace, it would be an immediate disaster if a quantum channel could change the trace of the input. This condition can be expressed mathematically as follows.

$$\mathrm{Tr}\left[M_A\right] = \mathrm{Tr}\left[\Phi\left[M_A\right]\right], \quad \forall M_A \in L(\mathcal{H}_A). \tag{15}$$

Complete positivity: The other essential property of a quantum state is that it is a positive semidefinite operator. So one might expect that our second condition for quantum channels should be that they must map PSD operators to PSD operators. However, this condition is called *positivity* and in fact is not strong enough. The issue arises when dealing with composite systems. Suppose our superoperator Φ, is trace-preserving and satisfies positivity, then any quantum state that we feed it as an input will indeed produce a quantum state. However, suppose we have a composite system and only act with Φ on part of our system, then this too should produce a quantum state. Such an operation is described by acting on the whole system with the following superoperator,

$$\Phi \otimes \mathcal{I}_C : L(\mathcal{H}_A \otimes \mathcal{H}_C) \to L(\mathcal{H}_B \otimes \mathcal{H}_C),$$

where $\mathcal{I}$ is the identity superoperator. It turns out that even if Φ satisfies positivity, $\Phi \otimes \mathcal{I}$ may still send PSD operators to non-PSD operators! The necessary condition then is complete positivity which deals with this issue in

[1] Actually we need to be slightly stricter than this as we are about to see

the following, somewhat hamfisted manner. A superoperator given by (14) is completely positive when,

$$\begin{aligned} (\Phi \otimes \mathcal{I}_C)[M] \in \mathrm{PSD}(\mathcal{H}_B \otimes \mathcal{H}_C), \\ \forall\, \mathcal{H}_C \;\text{ and }\; \forall M \in \mathrm{PSD}(\mathcal{H}_A \otimes \mathcal{H}_C). \end{aligned} \tag{16}$$

With these two conditions in hand, we are now prepared to define a quantum channel,

Definition 2. *A quantum channel is a superoperator,*$\Phi : L(\mathcal{H}_A) \to L(\mathcal{H}_B)$*, that is both trace-preserving and completely positive as defined in Eq. (15) and Eq. (16) respectively. Quantum channels are therefore often referred to as CPTP maps.*

While the above definition of a quantum channel is precise, it is a bit formal and does not offer much physical intuition. However, there are two equivalent ways of representing quantum channels that are much more intuitive and under their own set of conditions satisfy complete positivity and the trace-preserving condition. We turn to the first of these now.

2.2.1 Stinespring Representation

The Stinespring representation of quantum channels provides us with the most physical intuition by decomposing any channel into three different steps, each of which has a clear physical interpretation. The decomposition is as follows. We first start by taking the tensor product of our input state with some pure state. This obviously has a clear physical interpretation of adding a new particle to our system, a new qubit to our quantum computer, or something of that ilk. Next, we apply a unitary transformation to our new expanded system. As we know from standard quantum mechanics this is exactly how we describe the transformation of closed quantum systems, including but not restricted to the evolution generated by Hermitian generators. The last step is then to take a partial trace over some subsystem (not necessarily the recently added subsystem). Again this has an obvious interpretation of simply discarding part of our system. Putting this together the Stinespring representation of a quantum channel can be written as follows,

$$\Phi[\rho] = \mathrm{Tr}_E \left[U \left(\rho \otimes |\psi\rangle \langle\psi| \right) U^\dagger \right],$$

where if $\Phi : L(\mathcal{H}_A) \to L(\mathcal{H}_B)$, then $|\psi\rangle \in \mathcal{H}_C$ and $\mathcal{H}_A \otimes \mathcal{H}_C \cong \mathcal{H}_B \otimes \mathcal{H}_E$. We can also further compactify the Stinespring representation by noting that the act of adding a state and then acting unitarily can be achieved in one step by instead acting with an isometry. We can therefore instead write,

$$\Phi[\rho] = \mathrm{Tr}_E \left[V \rho V^\dagger \right], \tag{17}$$

where $V : \mathcal{H}_A \to \mathcal{H}_B \otimes \mathcal{H}_E$, and $V^\dagger V = I$. In fact, if we relax the isometry condition and allow V to be any matrix, the form of Eq. (17) automatically

guarantees the complete positivity of Φ. It is then the isometry condition that ensures that the map is also trace-preserving. The form of the Stinespring representation also has a clear analogy with the dynamics of open quantum systems. Since we can treat open quantum systems as being subsystems of a larger closed system, namely the subsystem and an environment, then the dynamics of the closed system can be described unitarily, and the resulting dynamics on the subsystem is obtained by taking the partial trace over the environment. This composition of operations is clearly in close analogy with the Stinespring representation [24].

2.2.2 Kraus Representation

While the intuition behind the Stinespring representation is very clear the need to constantly refer to an auxiliary system is quite computationally cumbersome. It would then be quite nice to be able to describe the action of a quantum channel on a system with reference to only that system. The Kraus representation has exactly this quality. The Kraus representation for a quantum channel $\Phi : L(\mathcal{H}_A) \to L(\mathcal{H}_B)$ is as follows,

$$\Phi[\rho] = \sum_{i=1}^{r} E_i \rho E_i^\dagger, \tag{18}$$

where the E_i's linear maps from $\mathcal{H}_A$ to $\mathcal{H}_B$. Just as with the Stinespring representation, a map of this form is already guaranteed to be completely positive, even without any constraints on the E_i's. It is quite easy to find what constraints the E_i's must satisfy so as to be trace-preserving. We simply need to take the trace of Eq. (18) which gives,

$$\begin{aligned} \mathrm{Tr}[\rho] &= \mathrm{Tr}\left[\sum_{i=1}^{r} E_i \rho E_i^\dagger\right] \\ &= \mathrm{Tr}\left[\sum_{i=1}^{r} E_i^\dagger E_i \rho\right], \end{aligned}$$

where we have used the cyclic property of the trace. Since this must be true for all inputs, ρ, the only possibility is that,

$$\sum_{i=1}^{r} E_i^\dagger E_i = I. \tag{19}$$

The set of operators $\{E_i\}$ are referred to as Kraus operators. It should be noted that a quantum channel does not have a unique choice of Kraus operators. However it is always the case that if,

$$\Phi[\rho] = \sum_{i=1}^{r} E_i \rho E_i^\dagger = \sum_{i=1}^{r} F_i \rho F_i^\dagger,$$

then the sets $\{E_i\}$ and $\{F_i\}$ are related unitarily. That is,

$$\sum_{j=1}^{r} U_{ij} E_j = F_i, \tag{20}$$

importantly the operation here is not matrix multiplication with U multiplying each E_i, but a unitary transformation on the vector that has the E_i's as its entries. While the Kraus representation is not unique this unitary relation does allow us to construct a unique orthogonal set, in the sense that,

$$\mathrm{Tr}\Big[E_i^\dagger E_j\Big] = f(i,j)\delta_{ij}. \tag{21}$$

Such a decomposition of a superoperator (or in particular a quantum channel) is equivalent to the eigendecomposition of an operator.

2.2.3 Choi Operator

So we have established two very useful representations of a quantum channel. However, supposing we are given some superoperator that acts as some sort of black box, in that we can input states and receive the output but we know nothing about the internal structure. How can we tell if this superoperator is a quantum channel or not? In fact, this can be checked quite easily. We simply need to feed it one half of a maximally entangled state (conventionally unnormalized)[2]. That is for some black box superoperator, Φ, we obtain,

$$J_\Phi = \sum_{i,j} (\mathcal{I} \otimes \Phi) \left[|ii\rangle \langle jj| \right] \in L(\mathcal{H}_A \otimes \mathcal{H}_B). \tag{22}$$

This object is referred to as the Choi operator of the superoperator Φ. The usefulness of the Choi operator lies in the fact that if Φ is completely positive, then J_Φ will be a positive semidefinite operator. Furthermore if Φ is trace preserving then, $\mathrm{Tr}_B[J_\Phi] = I_A$. Furthermore Eq. (22) defines an isomorphism from the Hilbert space of superoperators to the Hilbert space of operators. This isomorphism is referred to as the Choi-Jamiołkowski isomorphism [25, 26]. An important example is in the case that the quantum channel is unitary, then the Choi operator will be a maximally entangled pure state.

2.3 Entropy, Entanglement & Entanglement Entropy

2.3.1 Entropy

In information theory, both classical and quantum, entropy is a quantity of central importance. Given a probability distribution, the entropy of said distribution can be understood as a measure of our lack of knowledge for said distribution. For example, for a probability distribution that is highly concentrated we have close to complete knowledge about what outcome we can expect

[2] we shall discuss what is meant by maximally entangled shortly.

and so the entropy is low. Alternatively, for an evenly spread distribution, all outcomes will be equally likely and so, we have no knowledge about what outcome to expect. Therefore, the entropy is high.

This notion was first quantified in classical information theory with the *Shannon Entropy* [27], given by,

$$S(p) = \sum_i -p_i \log(p_i). \tag{23}$$

The generalization to quantum information theory is then straightforward and is called the *von Neumann Entropy*. Given a density matrix, ρ, the von Neumann entropy is given by,

$$S(\rho) = \mathrm{Tr}[-\rho \log(\rho)] = \sum_i -\lambda_i \log(\lambda_i), \tag{24}$$

where the λ_i's are the eigenvalues of ρ. The von Neumann entropy can also be viewed as the expectation value of the *Modular Hamiltonian*, $H_\rho = -\log(\rho)$, i.e.

$$S(\rho) = \langle H_\rho \rangle = \mathrm{Tr}[\rho H_\rho] \tag{25}$$

To see where the name comes from one can observe the similarity between the expression for ρ in terms of H_ρ and a thermal density matrix at inverse temperature β and Hamiltonian H,

$$\rho = e^{-H_\rho}, \ \rho_{th} = \frac{e^{-\beta H}}{Z}. \tag{26}$$

What follows are some important properties of the von Neumann entropy. For a density matrix ρ,

- $S(\rho) \geq 0$, and $S = 0$ if and only if ρ is pure.
- $S(\rho) \leq \log(\mathrm{rank}(\rho)) \leq \log(\dim \mathcal{H})$, the upper bound is saturated if and only if $\rho \propto I$, i.e. maximally mixed.
- $S(\rho) = S(V\rho V^\dagger)$, where V is an isometry, $V^\dagger V = I$.
- $S(\rho_A \otimes \rho_B) = S(\rho_A) + S(\rho_B)$
- **Subadditivity:** $S(\rho_{AB}) \leq S(\rho_A) + S(\rho_B)$, [28]
- **Strong Subadditivity:** $S(\rho_{ABC}) + S(\rho_A) \leq S(\rho_{AB}) + S(\rho_{AC})$, [29]

Another type of entropy that will be useful to us is the Renyi entropy which is given by,

$$S_\alpha(\rho) = \frac{1}{1-\alpha} \log(\mathrm{Tr}[\rho^\alpha]). \tag{27}$$

The Renyi entropy is monotonically decreasing in α and in the limit $\alpha \to 1$, produces the von Neumann entropy. The list of values of $S_\alpha(\rho)$ for all $\alpha \in \mathrm{N}$

is called the *entanglement spectrum*. Knowing the entanglement spectrum is equivalent to knowing all the eigenvalues of ρ. As we will see shortly the von Neumann entropy is not just a measure of information but in certain cases, can also be used as a measure of entanglement in a quantum state.

2.3.2 Entanglement

For multipartite quantum systems, we can classify the states of such systems according to the amount and type of correlation that exists between subsystems. The first class of states are the *product states*, which are of the form,

$$\rho = \rho_1 \otimes \rho_2 \otimes \cdots \otimes \rho_n. \tag{28}$$

These states are completely uncorrelated, a measurement outcome on one of the subsystems gives us no information about the other subsystems. The next class are known as *separable states*, these are statistical ensembles of product states,

$$\rho = \sum_i p_i \, \rho_{1,i} \otimes \rho_{2,i} \otimes \cdots \otimes \rho_{n,i}. \tag{29}$$

These states may contain classical correlations between subsystems, in the sense that for a pair of observables $\mathcal{A}_j$ and $\mathcal{A}_k$ supported on subsystems j and k, we have that,

$$\langle \mathcal{A}_j \mathcal{A}_k \rangle_\rho = \sum_i p_i \langle \mathcal{A}_j \rangle_{\rho_{j,i}} \langle \mathcal{A}_k \rangle_{\rho_{k,i}}. \tag{30}$$

Specifically, since the set of product states is clearly a subset of the set of separable states, then the set {separable}\{product} is the set of classically correlated states. While separable states encapsulate all the properties of classical correlation, they are still just a small subset of the possible quantum states on a multipartite system. The final class of states then are the *entangled states*. Entangled states are defined to be the non-separable states, i.e. {entangled} = {separable}$^{\mathrm{c}}$. These states contain correlation that is entirely quantum in nature. States of this kind were first discovered by Einstein, Podolsky, and Rosen [30], where they were used to argue for the incompleteness of quantum mechanics, in part because they seem to allow for instantaneous communication between spatially separated systems. However, we know today that this is not the case [31] and entangled states really do exist in nature. Unfortunately, there is no general expression for the form of entangled states as there is for the above cases, and indeed the task of determining whether some state is entangled or not is often NP-hard [32]. Thankfully however we will mostly be restricting our focus to entangled pure states. In this case and in particular in bipartite systems entanglement can be quite easily understood

2.3.3 Entanglement Entropy

We first note that if we restrict to only considering pure states, then all possible separable states are in fact just product states where the density matrices in

Eq. (28) are also pure. The definition of entangled states then also simplifies. An entangled pure state is any state that cannot be written in the form,

$$|\psi\rangle = \bigotimes_i |\phi_i\rangle \,, \tag{31}$$

where $|\phi_i\rangle \in \mathcal{H}_i$ and the dimensions of $\mathcal{H}_i$ need not be the same. If we now bipartition the system then the state can equivalently be written as,

$$|\psi\rangle = |\psi_A\rangle \otimes |\psi_B\rangle \,, \tag{32}$$

where $|\psi_A\rangle = \bigotimes_{i\in A} |\phi_i\rangle$ and $|\psi_B\rangle = \bigotimes_{i\notin A} |\phi_i\rangle$. We see that Eq. (32) is already in the form of a Schmidt decomposition with Schmidt rank, $r = 1$. Since we know that the Schmidt decomposition is unique, we can deduce that any bipartite state that has a Schmidt rank, $r > 1$ must be entangled.

An important feature of a pure product state is that its reduced density matrices are also pure, and so have zero entropy. What this is saying is that for a pure product state, it is possible to have perfect knowledge of a subsystem without knowing anything about the environment. The phenomenon of entanglement can somewhat roughly be understood as the delocalization of information in a quantum system. That is to say, in an entangled state, it is not possible to have perfect knowledge of a subsystem without knowing about the environment as well. We can formalize this idea by saying that the more entangled a bipartite pure state is the higher the entropy of its reduced density matrices will be i.e. the less we can know locally. In this context the entropy is known as the *entanglement entropy*. We will now motivate this idea with a few illustrative examples.

Schmidt rank: $r > 1$

We mentioned that any pure state with a Schmidt rank greater than 1 must be entangled, so let's now check the entropy of such a state, for example lets check the case where $r = 2$,

$$\begin{aligned} |\psi\rangle &= \sum_{i=1}^{2} s_i \, |a_i\rangle_A \, |b_i\rangle_B \,, \\ \rho_A &= \sum_{i=1}^{2} s_i^2 \, |a_i\rangle \langle a_i| \,, \\ S(A) &= -(p)\log(p) - (1-p)\log(1-p), \;\; 0 < p < 1 \end{aligned} \tag{33}$$

where to get to the third line we used the fact s_i^2 are the eigenvalues and since they must sum to one we can paramterize them by a single parameter, p. Note that p cannot be 0 or 1 as this would reduce to the $r = 1$ case. Futhermore, because ρ_A and ρ_B will always have the same eigenvalues, then $S(A) = S(B)$. This is a general feature of pure states. We can now deduce that $S(A)$ is always non-zero since $p = 0$ and $p = 1$ are the only roots of the expression. Furthermore,

the maximum of the entropy is at $p = 1/2$, for which $S(A) = \log(2)$. Indeed it can be shown that for any Schmidt rank r the maximum entropy is given by $\log(r)$.

Maximally entangled states

A maximally entangled state is a bipartite state of the form,

$$|\psi\rangle = \sum_{i=1}^{d} \frac{1}{\sqrt{d}} |a_i\rangle_A |b_i\rangle_B , \tag{34}$$

where d is the dimension of the smaller of the two Hilbert spaces. The reduced density matrix on the smaller of the two, let's say A, is then given by,

$$\rho_A = \frac{I}{d}, \tag{35}$$

from which it immediately follows that the entropy is the maximal, $S(A) = \log(d)$. It is in this sense that the state is maximally entangled. If we only have access to the smaller subsystem, we have no information about the state of that subsystem.

With these examples, it should be clear why entanglement entropy is a suitable measure of entanglement in bipartite pure states. It's important to note that since the entanglement entropy only depends on the Schmidt coefficients, it is impossible to increase the entanglement between the two subsystems by acting with a local unitary, as this will just change the basis used in the Schmidt decomposition won't affect the coefficients. Unfortunately, entanglement in general is much harder to measure, even in multipartite pure states. However, for our purposes, entanglement entropy will suffice.

See [33, 34] for more in depth discussion of many of the topics in this section.

3 Holography & the AdS/CFT correspondence

The birth of holography can be traced back to the 1970's when Bekenstein proposed that in order to reconcile the second law of thermodynamics with black hole physics a black hole must have an entropy [4]. Based on Hawking's earlier work [35] showing that the event horizon area is a strictly increasing quantity, Bekenstein proposed that the entropy is proportional to the horizon area. Hawking later strengthened this proposal [36] by investigating the behavior of quantum fields near the event horizon in a fixed black hole geometry. He found that with this inclusion of quantum mechanics, black holes are in fact thermal objects with an entropy that is indeed proportional to the horizon area,

$$S_{BH} = \frac{A}{4G}. \tag{36}$$

This discovery by Hawking, is today much more well known by the layman for the counter-intuitive suggestion that black holes are not black but in fact emit

Hawking radiation. However, the result that black hole entropy is proportional to the surface area is equally revolutionary. Thermodynamic entropy is understood to be an extensive property, in that it scales with system size, so an entropy being proportional to the surface area of a system was an entirely new phenomenon. In fact, if one were to demand that black hole entropy *is* extensive, then one is automatically lead to a rudimentary example of the *holographic principle*. That is, a black hole as seen by an external observer is holographically described by degrees of freedom defined on its horizon. This idea is dubbed the *central dogma of quantum black holes* in [37]. This was the first hint that a complete theory of quantum gravity might be holographic [2, 3].

Today holography is being found, more and more, to be naturally described within the language of quantum information theory, and it is exactly this information-theoretic approach that we will focus on. In this section we will first introduce the basics of black hole thermodynamics which will serve as a natural setup to discuss the entanglement area laws [9, 38, 39, 40] in the most successful instance of holography, the *AdS/CFT correspondence*[5].

3.1 Black hole thermodynamics

The first hint at some similarity between the laws of thermodynamics and the behavior of black holes can be seen even at a classical level when determining how a black hole responds to small amounts of matter falling into it. For example, if we drop a particle of mass ΔM and angular momentum ΔJ into the black hole, the event horizon will very quickly settle to a new larger surface area, with the change in area given by,

$$\frac{\kappa}{8\pi G_N}\Delta A = \Delta M - \Omega \Delta J, \tag{37}$$

where κ is the surface gravity and Ω is the angular velocity of the horizon. Following Bekenstein's reasoning, since the area is strictly non-decreasing, we posit that $\Delta A \propto \Delta S$. We will take a further leap and also take $T \propto \kappa$ (we shall vindicate this seemingly unfounded proposition shortly). After some rearranging this gives us,

$$\Delta M = T\Delta S + \Omega \Delta J. \tag{38}$$

This equation of course bears a striking resemblance to the first law of thermodynamics, and as such is often called the first law of black hole mechanics. Similarly, as discussed above Hawking showed [35] that classically,

$$\Delta A \geq 0, \tag{39}$$

which resembles the second law of thermodynamics. So it seems that even when treated classically the horizon area is governed by laws that are at least structurally similar to both the first and second law of thermodynamics. However, assuming temperature is proportional to surface gravity seems somewhat presumptuous, so maybe this analogy should not be taken too seriously. But, as we will now show when treated quantum mechanically black holes are thermal

objects with exactly $T = \frac{\kappa}{2\pi}$. To show this we will first derive the Fulling-Davies-Unruh effect, or more commonly just the Unruh effect[41, 42, 43]. Which will then imply the Hawking effect as a consequence.

3.1.1 Unruh Effect

The surprising claim of the Unruh effect is that this thermal behavior of the quantum vacuum is not special to black holes, but in fact is inherent to any observer undergoing non-geodesic motion, even in flat space. Furthermore, the temperature they experience is proportional to their proper acceleration. As we will see this thermal behavior is inextricably linked to the presence of a horizon. The trajectory of an object undergoing constant proper acceleration a is, in an inertial frame, parameterized in terms of proper time as,

$$x = \frac{1}{a}\cosh(a\tau), \quad t = \frac{1}{a}\sinh(a\tau). \tag{40}$$

In light-cone coordinates, $u = \frac{x+t}{\sqrt{2}}$, $v = \frac{x-t}{\sqrt{2}}$, the spacetime can be divided into four quadrants determined by the signs of u and v. These quadrants correspond to the causal past and future of the origin, as well as the left and right spacelike separated wedges. By expressing the accelerated trajectory in these new coordinates, $u = \frac{1}{a\sqrt{2}}e^{a\tau}$ and $v = \frac{1}{a\sqrt{2}}e^{-a\tau}$, it is clear to see that for positive a, the accelerated object is forever bound to the $(u > 0, v > 0)$ or the right spacelike wedge. Therefore an observer following such a trajectory would see an effective future and past horizon for $v = 0$ and $u = 0$ respectively. In the $t = 0$ Cauchy slice, when both the inertial observer and accelerated observer are stationary, we see that the origin acts as the horizon, which is a distance $1/a$ from the accelerated observer. Furthermore, the union of all such trajectories, Eq. (40), for positive a covers the right wedge, and since they are nonintersecting we can use them to define a new coordinate system for the accelerated observer, namely,

$$\rho = \frac{1}{a}, \quad \theta = a\tau. \tag{41}$$

Where $0 < \rho < \infty$ is the distance the accelerated observer measures to the apparent horizon and $-\infty < \theta < \infty$, the proper acceleration times the proper time is known as the rapidity. These coordinates are known as Rindler coordinates, and the $|t| < x$ wedge that they cover is called the right Rindler wedge. In terms of the Rindler coordinates the metric is of the form,

$$ds^2 = -\rho^2 d\theta^2 + d\rho^2. \tag{42}$$

With this in hand, we now determine the quantum vacuum in terms of the Euclidean path integral in both coordinate systems and compare. As usual, we first need to perform a Wick rotation, which we can achieve with $\theta = i\theta_E$, this has the following effect on the inertial coordinates,

$$\begin{aligned} x &= \rho\cos(\theta_E), \\ t &= i\rho\sin(\theta_E), \end{aligned} \tag{43}$$

which after a complimentary Wick rotation on the inertial coordinates, $t = it_E$, gives,

$$\begin{aligned} x &= \rho\cos(\theta_E), \\ t_E &= \rho\sin(\theta_E). \end{aligned} \tag{44}$$

As a result the metric given by,

$$\begin{aligned} ds^2 &= dt_E^2 + dx^2, \\ &= \rho^2 d\theta_E^2 + d\rho^2, \end{aligned} \tag{45}$$

Evidently, the Rindler metric now has the form of Euclidean polar coordinates. Under the assumption that the Hilbert space can be factorized into the left and right wedge we can determine the vacuum amplitudes as follows,

$$\left(\langle\phi_L| \otimes \langle\phi_R|\right)|0\rangle \propto \int_{t\to-\infty}^{\phi(t=0)=(\phi_L,\phi_R)} \mathcal{D}\phi e^{-S_E}, \tag{46}$$

where (ϕ_L, ϕ_R) is shorthand for $\phi(x) = \phi_L(x)$ for $x < 0$ and $\phi(x) = \phi_R(x)$ for $x > 0$. However since it is now clear that in Euclidean space ∂_θ generates rotations this path integral can equivalently written as,

$$\int_{t\to-\infty}^{\phi(t=0)=(\phi_L,\phi_R)} \mathcal{D}\phi e^{-S_E} = \int_{\phi(\theta=0)=\phi_R}^{\phi(\theta=-\pi)=\phi_L} \mathcal{D}\phi e^{-S_E}, \tag{47}$$

and from this equivalence we can determine that,

$$\left(\langle\phi_L| \otimes \langle\phi_R|\right)|0\rangle \propto \langle\phi_L|\exp(-\pi H_\theta)|\phi_R\rangle, \tag{48}$$

where H_θ is the Hermitian observable that generates translations in θ. We can finally then express the vacuum state in terms of H_θ,

$$|0\rangle \propto \sum_{L,R} \left(\langle L|\exp(-\pi H_\theta)|R\rangle\right)|L\rangle \otimes |R\rangle, \tag{49}$$

where $|L\rangle$ and $|R\rangle$ are bases for the left and right Hilbert spaces respectively. Since an accelerated observer only has access to the right Rindler wedge it then follows that this observer sees the vacuum as follows,

$$\begin{aligned} \mathrm{Tr}_L\left[|0\rangle\langle 0|\right] &= \frac{\exp(-2\pi H_\theta)}{\mathrm{Tr}\left[\exp(-2\pi H_\theta)\right]} \\ &= \frac{\exp\left(-\frac{2\pi}{a}H_\tau\right)}{\mathrm{Tr}\left[\exp\left(-\frac{2\pi}{a}H_\tau\right)\right]} \end{aligned} \tag{50}$$

where in the second line, we have simply converted back to the Rindler observer's proper time. Evidently, this is nothing more than a thermal state with temperature,

$$T = \frac{a}{2\pi} \tag{51}$$

which with constants restored is, $T = \frac{\hbar a}{2\pi k_B c}$. This is a different derivation from that originally used by Unruh, however this derivation emphasizes that the source of the thermal behavior is in fact the entanglement between the left and right Rindler wedges.

3.1.2 Hawking Effect

Having now derived the Unruh effect we can quite easily derive the Hawking effect with a simple implementation of the equivalence principle. To start with, the Schwarzschild metric is given by,

$$ds^2 = -\left(1 - \frac{r_s}{r}\right) dt^2 + \left(1 - \frac{r_s}{r}\right)^{-1} dr^2 + r^2 d\Omega_2^2, \tag{52}$$

where $r_s = 2G_N M$ is the Schwarzschild radius. Our goal is to show that for an observer hovering a constant small distance above the horizon, the spacetime is indistinguishable from Rindler space, i.e. flat spacetime as seen by an accelerating observer. We begin with the following change of coordinates,

$$\begin{aligned} \rho &= \sqrt{4r_s(r - r_s)} \\ \theta &= \frac{t}{2r_s} \end{aligned} \tag{53}$$

where, just as before, ρ is the distance to the horizon as measured by a stationary, near horizon observer and θ is the rapidity of said observer. After such a transformation the metric now has the form,

$$ds^2 = -\frac{4\rho^2 r_s^2}{4r_s^2 + \rho^2} d\theta^2 + \left(1 + \frac{\rho^2}{4r_s^2}\right) d\rho^2 + \left(r_s^2 + \frac{\rho^2}{2} + \frac{\rho^4}{16 r_s^2}\right) d\Omega^2, \tag{54}$$

which for $\rho \ll 1$ and the angular component suppressed becomes,

$$ds^2 = -\rho^2 d\theta^2 + d\rho^2. \tag{55}$$

As promised the near horizon spacetime for a static observer is indistinguishable from Rindler space, Eq. (42). We can therefore deduce that such an observer will feel a temperature $T(\rho \ll 1) = \frac{1}{2\pi\rho}$. To determine the temperature for large ρ we use the Tolman relation [44],

$$T(\rho)\sqrt{-g_{\theta\theta}(\rho)} = \text{const.} \tag{56}$$

We can determine that for small ρ the constant is $1/2\pi$. Therefore we have,

$$T(\rho) = \frac{1}{2\pi}\sqrt{\frac{4r_s^2 + \rho^2}{4\rho^2 r_s^2}}, \tag{57}$$

for all ρ and from here we can deduce that the Hawking temperature which is the temperature measured by an asymptotic observer is given by,

$$T_H = \frac{1}{4\pi r_s} = \frac{\kappa}{2\pi}, \tag{58}$$

just as we proposed at the start of the section. With reference to Eq. (37). We can fix the propotionality between A and S to obtain,

$$S_{BH} = \frac{A}{4G_N}. \tag{59}$$

If we restore the constants, $S_{BH} = \frac{k_B c^3 A}{4G_N \hbar}$, we see that we have the fundamental constants from general relativity, quantum mechanics and thermodynamics all working in unison. However, we run into a problem here, since black holes in fact radiate thermal energy, if nothing falls into the black hole then its mass will slowly radiate away and so its surface area will decrease. It seems then that Eq. (39) fails. However, the key insight here is that as the emitted Hawking radiation is in fact entangled with modes in the interior of the black hole, this is in exact analogy with the entanglement present between the left and right Rindler wedges in flat space. We must therefore include the entanglement entropy in our considerations. This provides us with the *generalized second law*[4],

$$\begin{aligned} S_{gen} &= \frac{A}{4G_N} + S_{out} \\ \Delta S_{gen} &\geq 0, \end{aligned} \tag{60}$$

where S_{out} is the entanglement entropy of the bulk fieds just outside the horizon.

3.2 the AdS/CFT correspondence

So far we have seen just hints of holography. However, the AdS/CFT correspondence provides a theory where it is exactly realized. In the original proposal [5] the correspondence was presented as a duality between a $3+1$ dimensional, maximally supersymmetric SU(N) Yang-Mills theory (a conformal field theory) and a $4+1$ dimesional anti de Sitter spacetime. This duality arose because in type IIB string theory a stack of N D3 branes creates a geometry near the branes that is $AdS_5 \times \mathrm{S}_5$. in the large N limit. The system, can therefore be described by semiclassical gravity on an AdS_5 background. However, it was already a well know fact in string theory that N coincident D branes represents SU(N) Yang Mills theory. Therefore, it must be the case that in the large N limit where both the AdS and the CFT descriptions are valid, that these two theories are equivalent! While the semiclassical AdS description is only valid at large N the Yang Mills description is valid for any value of N. It is therefore proposed that the duality holds for all N, where away from the large N limits the gravitational description moves away from the semiclassical limit and towards a full quantum gravitational system. Clearly, then AdS/CFT satisfies the holographic principle, since we have a $D+1$ dimensional theory of quantum gravity being equivalently described by a D dimensional qunatum field theory! Let's now give a brief outline of the important features of anti-de Sitter spacetime and conformal field theory before presenting a more precise statement of the correspondence.

3.2.1 Anti-de Sitter spacetime

AdS is a vacuum solution to the Einstein field equations such that the spacetime has negative cosmological constant. In metric is given by,

$$ds^2 = -\left(1 + \frac{r^2}{l_{AdS}^2}\right) dt^2 + \left(1 + \frac{r^2}{l_{AdS}^2}\right)^{-1} dr^2 + r^2 d\Omega_{d-1}^2, \tag{61}$$

where l is the AdS radius related to the intrinsic negative curvature created by the cosmological constant. The isometry group of the spacetime is $SO(d,2)$, which is isomorphic to the Lorentz transformations in $d+2$ dimensions. An important feature of AdS is that lightlike trajactories can extend to the boundary at spatial infinity and back again in finite proper time. Further still, any timelike trajectories will also return to their starting point in finite propertime, however they will not reach the asymptotic boundary. It is this quality that makes AdS somewhat like a gravitational system "in a box".

3.2.2 Conformal field theory

A conformal field theory is a quantum field theory with an extended group of spacetime symmetries, namely the Poincare group is extened to the conformal group. There are then, two new types of symmetries. The first type is Dilatations,

$$x^\mu \to \lambda x^\mu, \tag{62}$$

where λ is some real number. The second type are called special conformal transformations,

$$x^\mu \to \frac{x^\mu + a^\mu x^2}{1 + 2a_\nu x^\nu + a^2 x^2}. \tag{63}$$

The conformal group in $d+1$ dimensional spacetime is $SO(d+1,2)$, which is the Lorentz group of a spacetime with an extra space and an extra time dimension.

An important feature of CFTs are the primary operators. These are operators commute with special conformal transformations, and under Dilatations transform as,

$$\mathcal{O} \to \lambda^{-\Delta}\mathcal{O}, \tag{64}$$

where Δ is known as the conformal dimension of the primary. The descendents of a primary are defined as, $\partial^n\mathcal{O}$, and have conformal dimension $\Delta + n$. One of the reasons these operators are important is that for any CFT there exists a one to one correspondence between the set of all primaries and descendents, and a complete basis of the CFT Hilbert space. This feature is known as the state-operator correspondence.

3.2.3 Statement of the correspondence

A precise statement of the correspondence is then as follows [45].

Definition 3. *Any conformal field theory on an* $\mathrm{R} \otimes \mathrm{S}^{d-1}$ *background is dual to a theroy of quantum gravity on an asymptotically* AdS^{d+1} *spacetime, these theories are dual in the sense that their Hilbert spaces are isomorphic,*

$$\mathcal{H}_{CFT^d} \cong \mathcal{H}_{AdS^{d+1}}.$$

We will now give some important feature of the correspondence.

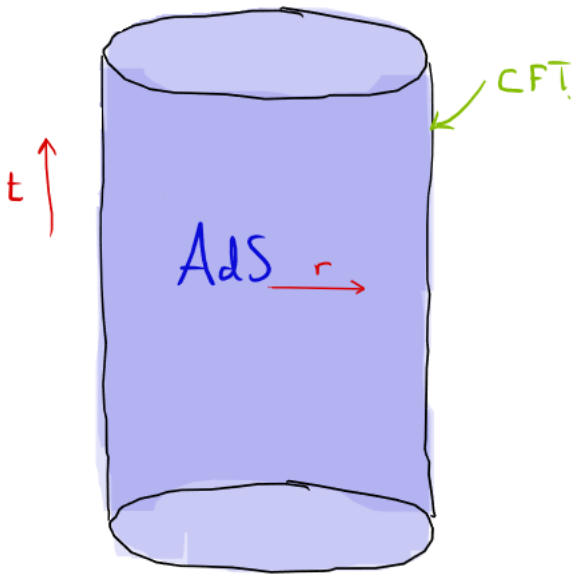

Figure 1: Here we have the bulk boundary correspondence illustrated for AdS_3/CFT_2. The CFT is defined on the surface of the cylinder while the AdS spacetime lives in the interior.

Bulk-Boundary: The CFT can be understood live on the asymptotic boundary of the spacetime. This follows from the extrapolate dictionary [46],

$$\mathcal{O}(t,x) = \lim_{r\to\infty} r^{\Delta}\phi(t,r,x), \tag{65}$$

where we see that a CFT primary, $\mathcal{O}$ with conformal dimension Δ can be represented by a bulk field ϕ in the limit of spacial infinity, and so the CFT operators are then defined at $r \to$ inf. We can then understand r as the emergent dimension. This concept is illusatrated in Fig. 1

Symmetries: The isometry group, the group of killing vector fields in the bulk, is isomorphic to the global symmetry group of the conformal field theory, $SO(d,2)$. Furthermore, generators of the CFT symmetry group get mapped to the generators of the AdS isometry group. In particular the CFT Hamiltonian gets mapped to the QG Hamiltonian and they have the same spectrum. Also the dilatation generator of the CFT gets mapped to the generator of translations r.

UV/IR: Since scaling transformations of the boundary correspond to translations in the radial direction in the bulk, imposing a cutoff on the bulk $r < r^*$ is equivalent to imposing a UV cutoff on the boundary. In this sense the short

range features of the boundary are encoded in the bulk at large r and the long range features are encoded at small r.

Thermal states: A thermal state of the CFT is dual to a black hole in AdS, where the temperature of the black hole is that of the CFT. In particular, at $T = 0$, i.e. the CFT vacuum, the corresponding bulk theory is the AdS vacuum solution.

Parameters: The CFT side of the duality is described by two parameters, the central charge, c, which can be seen as a counting of degrees of freedom ($c \sim N^2$), and the coupling strength λ. The AdS side of the duality has two parameters in the semiclassical limit, l_{AdS} and G_N and a third for string corrections l_S. The parameters of the two sides are then related by [47],

$$\begin{aligned} c &\propto \frac{(l_{AdS})^{d-1}}{G_N}, \\ \lambda &\propto \left(\frac{l_{AdS}}{l_S}\right)^{\gamma} \end{aligned} \tag{66}$$

3.3 Holographic Entanglement

As a consequence of the fact that thermal CFT states are dual to black holes in AdS we can make an immediate connection between holography and entanglement. We do this by constructing a purification of the thermal density matrix, which in this scenario is referred to as a thermofield double state,

$$\begin{aligned} \rho &= \frac{1}{Z} e^{-\beta H}, \\ |\mathrm{TFD}\rangle &= \frac{1}{\sqrt{Z}} \sum_i e^{-\beta E_i/2} \left|E_i\right\rangle \otimes \left|E_i\right\rangle, \end{aligned} \tag{67}$$

where $|E_i\rangle$ are the energy eigenstates and E_i the corresponding eigenvalues. What we have effectively done here however, is add another copy of the CFT and entangle it with our original. It is interesting to ask then if this state of the two CFT system also has a holographic dual. In [48] it was pointed out that this expansion of the CFT system is exactly analogous to going from the one sided black hole spacetime, to the maximally extended black hole spacetime. See Fig. 2. In this exteneded spacetime the two CFTs are then defined on each of the boundaries. In going from the density matrix to the thermofield double we have recast the thermodynamic black hole entropy as an entanglement entropy between the two CFTs. This is immedietley telling us something important about entanglement in holographic theories. The entanglement seems to generate spacetime geometry [49]. To justify this claim, consider the state $|E_i\rangle \otimes |E_i\rangle$. This state would simply correspond to two disconnected static spacetimes, and indeed so does every term in the superposition forming the thermofield double.

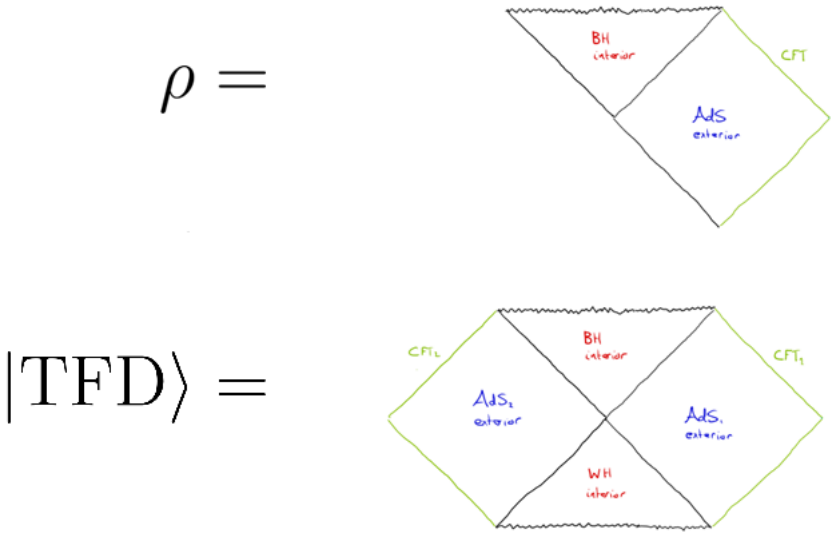

Figure 2: Here we show the analogy between constructing the thermofield doulbe of a CFT and extending the blackhole metric to the two sided maximally extended case

However, once these spacetimes are put in a superposition they become connected through a wormhole with horizon area proportional to the entanglement entropy. We will now present a series of increasingly general proposals for the connection between boundary entanglement and bulk geometry.

3.3.1 Ryu-Takayanagi proposal

The Ryu-Takayanagi proposal [9] was the first work that formalized the connection between entanglement and geometry, it can be seen somewhat as a generalization of the Bekenstein-Hawking entropy within AdS/CFT. The proposal is as follows.

- For a particular Cauchy slice, Σ, of the boundary CFT, there is a corresponding state, ρ_Σ. Assuming that the state is time reversal-symmetric and that the Hilbert space can be factorized into two complementary spatial regions A and $\bar{A}$ then we identify the entropy of the reduced density matrix, $\rho_A = \mathrm{Tr}_{\bar{A}}[\rho_\Sigma]$, with,

$$S(A) = \min_{\gamma_A \sim A} \left(\frac{|\gamma_A|}{4G} \right), \tag{68}$$

  where γ_A is a bulk curve, $|\dot{|}$ denotes the area and $\gamma_A \sim A$ means γ_A is homologous to A, that is, together γ_A and A form the boundary of hypervolume.

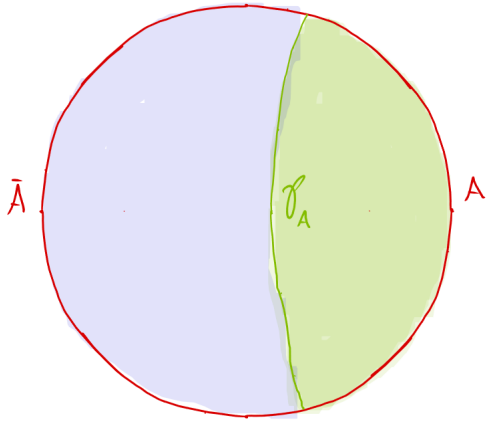

Figure 3: A time reversal-symmetric Cauchy slice of the boundary theory has been partitioned into A and $\bar{A}$. The minimal surface homologous to A is shown partitioning the bulk. For a pure state the area of this curve quantifies the entanglement between A and $\bar{A}$

So what the proposal is saying is that the entropy of a boundary subregion is proportional to minimal area of a bulk surface homologous to the the boundary subregion. In the case of pure bounary states the homology condition will reduce to the condition that γ_A and A share a boundary, in this case the entropy is an entanglement entropy, and example is shown in Fig. 3. In the case of mixed states however the homology condition is necessary. For example in the case of a thermal state the minimal surface for the entire boundary is exactly the event horizon of the black hole in the bulk.

Note however that this proposal is only valid for time reversal-symmetric slices. We would like then a more general, covariant prescription for obtaining the entropy. Furthermore, this expression is to be understood as only valid in the large N limit. That is the area contribution is the leading order term in a $1/N$ expansion for the entropy.

3.3.2 HRT proposal

Shortly after the RT proposal, it was generalized to a covariant version by Hubeny, Rangamani and Takayanagi [38]. The generalization is relatively straight forward. We must now find a surface homologous to our boundary region that is *extremal* with respect to infinitesimal deformations of the surface. If more than one extremal surface exists then the surface with the smallest area is selected. It is straightword to see that in static spacetimes this reduces to the RT propsoal since the RT surface is minimal with respect to spatial variations and maximal with respecet to timelike variations. In this maximin quality leads naturally to an equivalent statement of the HRT proposal[50].

- For a particular Cauchy slice, Σ_b, of the boundary CFT, there is a family of different bulk Cauchy slices,Σ_B, that asymptote to Σ_b. To determine the entropy of a reduced density matrix on a boundary region, $A \subset \Sigma_b$, we determine first determine the minimal surface homolgous to A for each of the bulk Cauchy slices Σ_B and then determine the RT entropies of these surfaces. The HRT surface and so the true entropy of the region is then given by the maximum of these entropies.

$$S(A) = \max_{\Sigma_B | \partial\Sigma_B = \Sigma_b} \left(\min_{\gamma \subset \Sigma_B \& \gamma \sim A} \left(\frac{|\gamma|}{4G} \right) \right) \tag{69}$$

3.3.3 Quantum Extremal Surfaces

We mentioned already that the RT formula for the entropy is just the leading term in a $1/N$ expansion. This of course is true for the HRT formula as well. How then can we include corrections to our expression? This question was answered in [39] and a subsequent a proposal for all orders was given in [40]. The proposal states that the entropy of a subregion is obtained by finding the surface that extremizes the bulk generalized entropy Eq. (60) as opposed to to just the area, where the S_{out} term is to be understood as the entropy of the bulk reduced density matrix on the region bounded by A and this extremal surface.

$$S(A) = \max_{\Sigma_B | \partial\Sigma_B = \Sigma_b} \left(\min_{\gamma \subset \Sigma_B \& \gamma \sim A} \left(\frac{|\gamma|}{4G} + S_{bulk}(\Sigma_\gamma) \right) \right), \tag{70}$$

where $\partial\Sigma_\gamma = A \cup \gamma$.

3.3.4 Entanglement wedges

An interesting question about these boundary subregions we have been dealing with is, given only the reduced density matrix of a boundary region, A, how much of the bulk can we reconstruct? The answer to this question is something called an *entanglement wedge* [51, 52, 50, 53, 54]. The entanglement wedge for a boundary region A is given by the domain of dependence of any spacelike surface that is bounded by the extremal surface. That is,

$$\mathcal{W}(A) = D_{bulk}(\Sigma_\gamma), \tag{71}$$

as shown in Fig. 4. The important feature of an entanglement wedge is that any local bulk operator in $\mathcal{W}(A)$ can be reconstructed on the boundary A in terms of some non-local CFT operator[55]. An intereting consequence of this however is that since a single spacetime point can be in the entanglement wedge of many different regions, this implies that a local bulk operator can be reconstructed in many different ways on the boundary. This unintuiative property of the AdS/CFT correspondence is a direct consequence of the quantum error correcting properties of the duality [10].

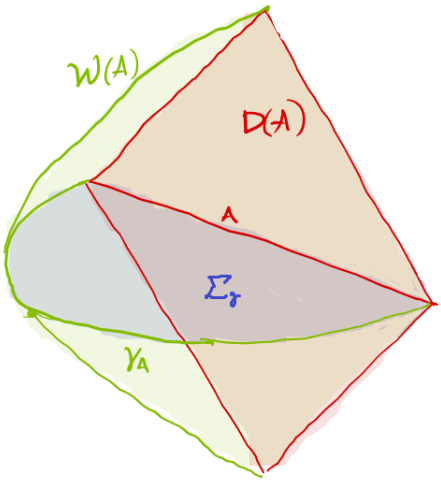

Figure 4: For the boundary region A (red), we have the entanglement wedge $\mathcal{W}(A)$ which is the bulk domain of dependence of Σ_γ (blue).

4 Tensor Networks

Having reviewed the basics of quantum information theory and Holography we will now introduce the starring role of this thesis, tensor networks. The current section will be dedicated to explaining what exactly a tensor network is, as well as introducing some particularly successful examples, with a focus on MERA networks.

4.1 What is a tensor network?

Tensor networks are a method for constructing approximations to large tensors by contracting together a number of smaller tensors. This method naturally facilitates a graphical representation as a network, where the nodes of the network are the tensors themselves and the edges represent the specific pattern of contraction. The main qualities of this approach that make it so attractive are twofold. Firstly, they allow for a huge reduction in the number of free parameters of the object of interest, allowing for many objects previously outside the scope of numerical computation to be tackled. Secondly, by using a tensor network representation, the network structure can often be chosen such that certain properties which might typically be hard to visualize are made more manifest. For example, the entanglement structure of many-body wavefunctions, as we shall see shortly.
Tensor Networks were originally utilized by the condensed matter community as a tool to approximate ground states of many-body systems[56]. However they have since proven invaluable across many fields including quantum information theory, lattice gauge theory [57], quantum chemistry [58] and even in computer

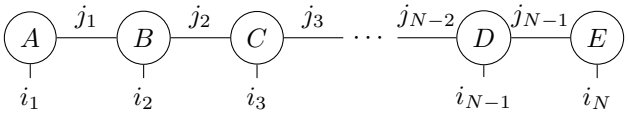

Figure 5: This is the tensor network graphical representation of Eq. (73), a matrix product state. The open legs represent uncontracted indices, while the legs which are attached to a tensor on both ends represent contracted indices.

science they have found use in the study of neural networks[59]. And lastly of course, they have been recently been proposed as a method to understand quantum gravity and holography[11].

For concreteness we shall henceforth restrict our discussion of tensor networks to those representing quantum states on Hilbert spaces of many factors.
Suppose we are interested in a particular wavefunction, such as the ground state, of a lattice system with N sites. Then for a particular T the wavefunction is given by,

$$|\psi\rangle = \sum_{i_1=1}^{d} \sum_{i_2=1}^{d} \cdots \sum_{i_N=1}^{d} T^{i_1 i_2 \cdots i_N} |i_1 i_2 \cdots i_N\rangle \,. \tag{72}$$

It should be clear that such a wavefunction, being an element of $\bigotimes_j^N \mathcal{H}_j$, is by definition a rank N tensor. It is also apparent that as N increases the number of amplitudes required to describe the state is d^N. This exponential scaling makes simulating even moderately sized quantum systems on a classical computer unfeasible.

As mentioned above, tensor networks generate an approximation of the true wavefunction by decomposing the high rank tensor into many low rank tensors and contracting over auxiliary indices. Using (72) as an example, we can represent T by a chain of smaller tensors as follows,

$$T^{i_1 i_2 \cdots i_N} = A^{i_1}_{j_1} B^{i_2}_{j_1 j_2} C^{i_3}_{j_2 j_3} \cdots D^{i_{N-1}}_{j_{N-2} j_{N-1}} E^{i_N}_{j_{N-1}}, \tag{73}$$

where Einstein notation is employed. Even for a relatively simple pattern of contractions such as this the notation is already quite cluttered. However when represented as a network, as in Fig. 5, it is much cleaner and more intuitive. Let's now count the number of parameters for each representation. As discussed the original wavefunction is described by d^N complex numbers. In our tensor network representation, we can assume for simplicity that each of the contracted j indices has dimension χ, which is referred to as the *bond dimension*. Then the two tensors on the ends of the chain have $d\chi$ parameters, and the $N-2$ other tensors have $d\chi^2$ parameters, and so the total number of parameters is $2\chi d + (N-2)\chi^2 d$. Evidently then the original wavefunction requires $\mathcal{O}(d^N)$ parameters, while the given tensor network approximation requires $\mathcal{O}(N)$.

So we have shown that by employing such a tensor network we can greatly reduce the number of free parameters. However, we as of yet have no reason to believe that such a structure is capable of providing a suitable approximation to quantum states. In fact (73) and Fig.5 is an example of the well known class of tensor network known as *Matrix Product States* (MPS). As we will see these networks are very well suited to do dealing with gapped 1D systems.

4.1.1 Constructing a Matrix Product State

Suppose we know exactly an N-body state given by $\psi^{i_1 i_2 \dots i_N}$, to build an MPS approximation, we start by grouping the first $N/2$ indices into a single composite index and act similarly for the remaining indices,

$$\psi^{i_1 i_2 \dots i_N} \to \psi^{IJ},\ I = i_1 i_2 \dots i_{N/2},\ J = i_{N/2+1} i_{N/2+2} \dots i_N. \tag{74}$$

In this way we have reshaped our quanutm state into a typical matrix, which allows us to perform the next step which is to perform a singular value decomposition or equivalently a Schmidt decomposition.

$$\begin{aligned} \psi^{IJ} &= \sum_K U^{IK} D^{KK} V^{KJ} \\ &= U^{IK} \tilde{V}^{KJ}, \end{aligned} \tag{75}$$

where D is a diagonal matrix containing the singular in descending order, and in the second line we have absorbed D into V. We can now iterate this process and decompose the resulting matrices until we have a single tensor per physical index. What we have obtained is an exact representation of the state in the form of an MPS network. However, we placed no upper bound on the bond dimension χ, meaning there is so far no computational advantange to this representation. To impose a particular bond dimension we must truncate the matrices at each decomposition step as follows. Using (75) as example we perform the following alteration,

$$\psi_{IJ} \to \sum_{K=1}^{\chi} U'^{IK} D'^{KK} V'^{KJ}, \tag{76}$$

where D' is again a diagonal square matrix but has now been truncated to be $\chi \times \chi$ matrix containing the χ largest singular values, similarly U' and V' are now isometries containing the first χ columns and rows of their counterpart respectively. By holding onto the largest singular values we maximize fidelity with the orignal state under such a truncation. This truncation can obviously be implemented at each iteration of the decompostion, and by the end we will obtain exactly a network as in Fig. 5 with the desired bond dimension. Lets now discuss some properties of MPS that should be evident after the above construction

Entanglement Entropy Since the MPS is constructed as a series of truncated SVD's the entanglement entropy of a subregion has an upper bound of

$\log(\chi)$, regardless of region size. This is exactly the entropy scaling (or lack there of) we expect for the ground states of gapped 1D systems! [60]

MPS states span Hilbert space As we saw from our construction we can start with any state in our many-body Hilbert space and construct an MPS network that represents it exactly as long as we don't truncate the singular values. In other words in the $\chi \to \infty$ limit the ansatz of MPS states spans the entire space, and as we decrease χ we target the corner of Hilbert space that contains gapped 1D ground states.

MPS underlies DMRG The density matrix renormalization group (DMRG) has been one of our best tools for classical simulation of 1D quantum systems since it's inception[56], and in fact can be viewed as a variational algorithm that finds the MPS state of minimum energy for a given Hamiltonian. The success is a consequence of the efficiency of MPS states as well as the low computational cost of determining correlators and expectation values.

4.1.2 Geometrization of Entanglement

So far we have introduced the simplest class of tensor network, the matrix product state, which as a consequence of its entropy scaling, we have seen is particularly well suited to describing the ground states of gapped 1D systems. However as we explored in section 2, different classes of quantum systems have different area laws. We can therefore expect that for systems with more involved area laws we will need different tensor network structures.
An immediate example is that of higher dimensional systems. Even without entanglement arguments it is obvious that MPS has an inherent 1D structure, and so cannot handle higher dimensional systems. The generalization is quite intuitive, we again assign a single tensor per site and contract auxiliary indices with neighbouring tensors leaving one uncontracted physical index per tensor. As a result we have a tensor network with the structure of a net as opposed to a chain. Such tensor networks are refered to as *projected entanglement pairs* (PEPS). See Fig. 6. While these networks share a structural similarity to MPS their properties are quite different. The fact that MPS states follow from a sequence of SVDs means that MPS states come equipped with a canonical form. However, due to the more intricate structure of PEPS networks, these decompositions are no longer in our toolbox. In fact, this is a property of any network structure that, like PEPS, contains closed loops. Additionally calculations of exact scalar products of PEPS states, and so also computing correlators, is exponentially hard. It is therefore necessary to implement additional approximations.
Despite these issues, it is true that PEPs states satisfy higher dimensional area laws. This can be seen quite easily by considering for example a 2D PEPS. If we are interested in the entanglement entropy of a particular region, it is quite clear that it is upper bounded by the number of contracted legs that cross the

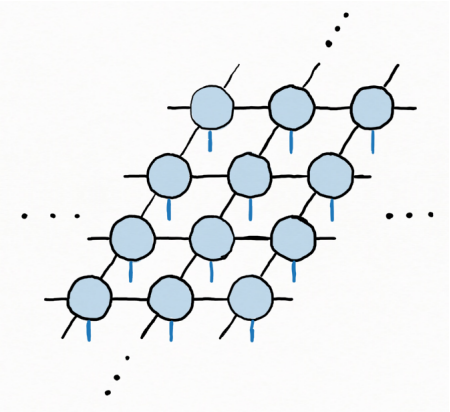

Figure 6: Here we have shown a small region of a PEPS network where the blue legs are the degrees of freedom of the system.

regions bounding surface, i.e. for some region A whose boundary ∂A intersects n legs then the entanglement is bounded as follows,

$$S(A) \leq n \log \chi = c(a)|\partial A| \log \chi, \tag{77}$$

where is c is the number of legs per unit area which depends on the particular lattice spacing a. Evidently then by taking quite logical generalizations to PEPS, we can in theory target the low energy eigenstates of gapped systems in any dimension.

Critical systems, however, have a logarithmic correction to the area laws of gapped systems. How then, can we build tensor networks that exhibit this property? In answering this question we can leverage the fact that critical systems have an additonal symmetry, scale invariance, to our advantage. The idea then is to build a tensor network, that mimics the action of a real-space renormalization group flow. The RG scheme that lends itself best to a tensor network representation is that of Kadanoff's block spin transformation [61]. Let's first make a naive attempt to construct such a network. In investigating the flaws of this naive attempt we will gain some indication of what refinements are neccessary.

The block-spin procedure is a very intuitive description of a renormalization transformation. Given a quantum system defined on a lattice (for concreteness we will work within the 1D case), the idea of Kadanoff is to partition our lattice into blocks of neighbouring sites and then replace each block with a single effective site in a new coarse-grained lattice. The result of this is that we should obtain an effective theory for our original system that overall has less degrees of freedom. Again, for concreteness, let's restrict to the particular case of 2 to 1 blocking, i.e. each of our blocks before coarse-graining contains two lattice

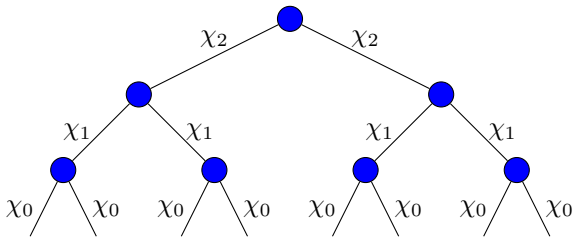

Figure 7: A simple example of a tensor network representation of a block spin RG flow. Here the chain is partitioned into blocks of two spins and χ_i represents the bond dimension of the spin chain after i renormalization steps.

sites[3]. Assigning to each site in our initial lattice a local Hilbert space $\mathcal{L}_i^0$, the Hilbert space of our full system is then given by,

$$\mathcal{H}^0 = \bigotimes_i \mathcal{L}_i^0. \tag{78}$$

The Hilbert space of a single block is then given by,

$$\begin{aligned} \mathcal{B}_j^0 &= \mathcal{L}_{2j}^0 \otimes \mathcal{L}_{2j+1}^0, \\ \implies \mathcal{H}_0 &= \bigotimes_j \mathcal{B}_j^0 \end{aligned} \tag{79}$$

Our coarse-graining proceedure is then naturally described by the isometric tensors V_i defined as follows,

$$V_i^\dagger : \mathcal{B}_i^0 \to \mathcal{L}_i^1,\ V_i^\dagger V_i = I \tag{80}$$

where $\mathcal{L}_i^1$ are the local Hilbert spaces of our new effective system, $\mathcal{H}^1 = \bigotimes_i \mathcal{L}_i^1$. We denote the dimension of the local Hilbert space at each iteration as $\chi_i = \dim \mathcal{L}^i$ with the $\chi_0 = d$, the local dimension of the original system. We can now iterate this process to obtain an increasingly coarse-grained system, until we have a bipartite system,

$$\mathcal{H}^0 \to \mathcal{H}^1 \to \cdots \to \mathcal{H}^n = \mathcal{L}^n \otimes \mathcal{L}^n. \tag{81}$$

Such a process is naturally represented by a tensor network, as shown in Fig. 7. This block spin inspired tensor network belongs to a class of tensor networks known as *tree tensor networks* (TTN), which are those networks that do not have closed loops (therefore including MPS).

Having made our naive attempt at building an RG inspired tensor network to tackle critical systems, let's now see why it fails. First of all the network is clearly translationally unsymmetric. Taking Fig. 7 as an example if we assume that the system has periodic boundary conditions then we have a $\mathbb{Z}_2$ translational

[3]Typically the blocks are equal size, but this is not strictly necessary

symmetry. This is obviously a big disadvantage when tackling systems with translational symmetry which we often are. Second if we wish to obtain any computational advantage from this representation we must impose an upper bound on the bond dimensions χ_i. If we therefore set all bond dimensions (not including uncontracted legs) to some universal χ, we will as usual obtain some reduction in free parameters. However as a consequence we now have that for regions of size 2^n, there will always be some region of this size that is connected to its complementary region through the network by a single leg. This means that we have an approximately constant entropy scaling, just like in MPS case.

So, what went wrong here? In answering this question we will meet for the first time the staring role of this thesis. That is, the *muliscale entanglement renormalization ansatz* (MERA). We will delve into a full exploration of this tensor network ansatz in the next section, but for now let's reflect on what we have learned about tensor networks and in particular how they relate entanglement to geometry.
Entanglement is often depicted in popular science as some unusual string like object connecting particles over large spatial separations. While no serious physicist should take this image of entanglement seriously, what tensor networks provide us with is a somewhat analogous way of graphically representing the entanglement structure of quantum states. The existence of entanglement in a quantum state is really the root cause of the exponential growth of the parameters required to describe the state. If we consider a state with no entanglement at all which in a lattice system with N sites corresponds to an N-fold product state, we only need $O(dN)$ parameters to describe the state. Contrary to this a generic state in the Hilbert space requires $O(d^N)$ parameters. However, we are often interested in states that have a very particular entanglement structure, for example local ground states which we have shown satisfy entanglement area laws. What tensor networks achieve, is the construction of a structure that requires less overall parameters to describe than a generic states while restricting to classes of states that have a specific entanglement structure. As we have seen the amount of entanglement between two regions is limited by the dimension of the composite Hilbert space of the minimal number of legs in the network that connect the two regions. This is very analogous to a fluid flowing through a system of pipes where the internal contracted indices play the role of the pipes and entanglement plays the role of the fluid. We have seen in PEPS, that the necessary network geometry responds directly to changes in the system geometry (change of dimension). However this is not sufficient to describe states with different entanglement structure like those of critical systems. As we will see in the next section, it is exactly the failure to properly account for entanglement that was the downfall of our initial attempt to build a tensor network for critical states.

4.2 Entanglement Renormalization

We now introduce the multiscale entanglement renormalization ansatz. Just as our tree tensor network in the section above was built to replicate Kadanoff's block spin RG transformation, MERA is based on a new real-space renormalization group transformation that is quite similar but importantly pays more careful attention to the entanglement in the state. This new RG scheme is refered to as *entanglement renormalization*.

Entanglement renormalization was first proposed by Vidal in [14]. The key realisation of Vidal that lead to this proposal, is that in the standard block spin approach, there is a failure to consider the entanglement between neighbouring blocks before they are coarse-grained. This neglect of short range entanglement is ultimately the reason that we can not expect a decent approximation for moderate bond dimension. He therefore introduced a new type of tensor dubbed the *disentangler*. The role of the disentanglers is to remove short range entanglement between neighbouring blocks before the *isometries* of the usual block spin procedure are applied. Exploring this more explicitly, we have as before our initial Hilbert space described by (78), which again we partition into two site blocks,

$$\mathcal{H}^0 = \bigotimes_j \mathcal{B}_j^0. \tag{82}$$

We then choose the disentanglers to be unitary operators that act on adjacent pairs of sites that traverse the border between our blocks. Choosing for illustration, a particular block $\mathcal{B}$, we label the lattice sites directly adjacent to $\mathcal{B}$ as α_1 and α_2, and label the lattice sites within $\mathcal{B}$ as β_1 and β_2. The disentanglers that act on $\mathcal{B}$ are then defined as,

$$\begin{aligned} u_1 &: \mathcal{L}_{\alpha_1}^0 \otimes \mathcal{L}_{\beta_1}^0 \to \mathcal{L}_{\alpha_1}^0 \otimes \mathcal{L}_{\beta_1}^0,\ u_1^\dagger u_1 = u_1 u_1^\dagger = I, \\ u_2 &: \mathcal{L}_{\beta_2}^0 \otimes \mathcal{L}_{\alpha_2}^0 \to \mathcal{L}_{\beta_2}^0 \otimes \mathcal{L}_{\alpha_2}^0,\ u_2^\dagger u_2 = u_2 u_2^\dagger = I. \end{aligned} \tag{83}$$

The goal in choosing our particular disentanglers is to minimize the amount of short range entanglement between $\mathcal{B}$ and its environment, or equivalently reduce the entropy of the reduced density matrix on $\mathcal{B}$. Defining the reduced density matrix on $\mathcal{B}$ and it's neighbouring sites as $\rho_{\alpha_1\beta_1\beta_2\alpha_2}$, the reduced density matrix on $\mathcal{B}$ after the disentanglers is then given by,

$$\rho'_{\beta_1\beta_2} = \mathrm{Tr}_{\alpha_1\alpha_2}\left[(u_1 \otimes u_2)\rho_{\alpha_1\beta_1\beta_2\alpha_2}(u_1^\dagger \otimes u_2^\dagger)\right]. \tag{84}$$

So the correct choice of u_1 and u_2 are those that minimize the entropy of $\rho'_{\beta_1\beta_2}$. There a multitude of ways of achieving this. One can treat the entropy of $\rho'_{\beta_1\beta_2}$ as a functional, $S : SU(4) \otimes SU(4) \to \mathbb{R}^+$, and use optimization techniques to find the minimum [20]. Other more sophisticated gradient descent methods have been explored in [62], in this case the energy expectation value is used as the cost function. It should be noted that the entropy will in most cases will never go to zero as we are only removing the short range entanglement.

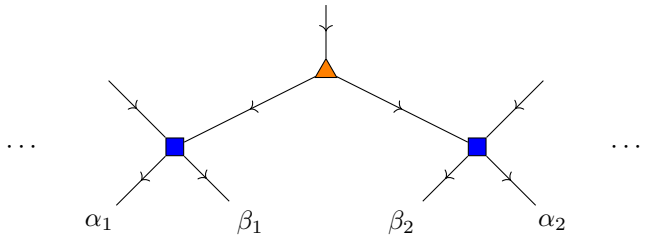

Figure 8: Shown is the tensor network containing those tensors that act on a particular block, $\mathcal{B}$, within a single entanglement renormalization iteration. The orange tensor represents the isometry while the blue tensors represent the disentanglers. Indices β_1 & β_2 are the indices of $\mathcal{B}$ while α_1 & α_2 are the immediately adjacent indices.

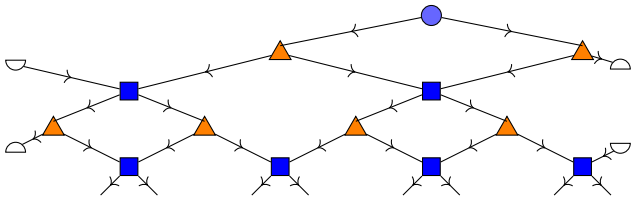

Figure 9: Tensor network representation of a 2 to 1 entanglement renormalization process. Here the system of interest is spin chain of eight spins with periodic boundary conditions. In each iteration, the disentanglers (blue squares) first remove entanglement between neighbouring blocks and the isometries (orange triangles) then map the blocks to a single effective spin. After two iterations the process terminates at the top tensor (blue circle). The white semi-circles indicate edges that pass over the periodic boundaries.

After similarly applying disentanglers to the boundaries of all blocks we can proceed with the coarse-graining. As before this is done by applying 2 to 1 isometries to our blocks, with isometies again defined by (80). The composition of disentanglers and isometries then constitutes a single iteration of the entanglement renormalization transformation. If we started with a chain of N sites, then after a single iteration we have a coarse-grained chain of $N/2$ sites (in the 2 to 1 case). The local Hilbert space dimesnion, χ, of this new chain may be larger than the original dimenion, d, and this χ corresponds to the bond dimension as before. A small section of the resulting network, centred around a single block is shown in Fig. 8 We can now iterate this process by applying a sequence of these ER layers to our chain, obtaining an increasingly coarse-grained chain at each step, see Fig. 9. For finite systems we will eventually obtain a chain of only two sites, at which point we insert a bipartite quantum state, thus closing all legs bar those of the physical system, this state is refered to as the *top tensor*. For a chain composed of 2^n sites, it evidently take $n-1$ ER layers to reach the top

tensor. Additionally, as with all tensor networks the parameter that controls both the computational cost of simulation and accuracy of approximation is the bond dimension χ. If we start with an initial local dimension of d the first ER iteration is capable of producing a coarse-grained chain with local dimension of up to χ^2. The same is true of all layers, that the maximum local dimension of the resulting chain is given by $\chi_{n+1} = \chi_n^2$, where n denotes the number of ER iterations already applied. Therefore if we wish to construct a network with dominant bond dimension χ, we will need at least $\log(\chi) - 1$ transitional ER layers that succesively increase the local dimension, at which point all remaining layers have a fixed dimesnion χ. The collection of all states that can be formed in this way for different choices of disentanglers and isometries forms a variational ansatz known as the *multiscale entanglement renormalization ansatz* (MERA) and algorithms have been establsihed by Vidal [63] to find the best approximation to Hamiltonian ground state within this ansatz.

Now that we have introduced the MERA class of tensor networks, lets investigate if they have truly triumphed over our previous attempt at representing 1D critical systems[4]. First of all it is immediately apparent that MERA networks contain a much higher degree (though not exact) of translational symmetry in their structure, this can be seen as a consequence of the disentanglers stitching the network together. However, this does come at a cost since our network now contains closed loops, and as mentioned earlier this means we can now longer use the Schmidt decomposition to find a canonical form for our network. In fact MERA networks contain a very large amount of gauge freedom. This can be seen quite clearly by inserting a unitary and its inverse on any leg and then absorbing one each of these tensors into the definition of the neighbouring disnentangler and isometry. This action will obvious not change the output state but our network is now different. This issue of gauge freedom and finding canonical forms will be very important in the holographic interpretation and we will return to this issue later.
Next, we discuss the original motivating point, the scaling of entanglement entropy. It was shown numerically by Vidal in his original paper [14], that entanglement entropy does indeed scale as expected for critical systems,

$$S(L) = \frac{c}{3}\log(L), \tag{85}$$

where c is the central charge of the continuum limit CFT. Heuristically, this logarithmic scaling can be understood as a consequence of the inherent logarithmic structure of the network itself. When we later explore the holographic properites of MERA we will give a more analytic exploration of the entanglement entropy.

So MERA networks are indeed capable of exhibiting critical entanglement entropy scaling, just as we set out to achieve, but this is far from the strength of

[4]In fact our earlier attempt is a special case of a MERA network where all disentanglers are constrained to be the identity

this ansatz. In particular, as a consequence of the all the tensors in the network being isometric, the expectation values of local observables can be computed extremely efficiently. This is a consequence of the fact that in contracting the network with the observable and the conjugate network will result in many of the tensors cancelling out. We therefore only have to consider a small subset of the tensors in our calculations when computing local observables.

5 Holographic Tensor Networks

5.1 Holographic MERA

Some connections between MERA and holography should at this point already be apparent. Both permit a $D+1$ dimensional representation of a D-dimensional system, and both can be understood as a geometrization of the entanglement in a quantum state. This apparent analogy lead Swingle to propose [11] that MERA may be used as a toy-model for holography and may give insight into holography beyond AdS/CFT. The idea is to view the network structure, which necessarily has a hyperbolic geometry as a discrete analogy of the emergent AdS spacetime, and to view the quantum state defined on the boundary as an approximation of the CFT state.

We next expand on this proposal and give some more concrete arguements in it's favour. We will denote the full network as $\mathcal{M}$ and the boundary, on which the quantum state is defined, as $\partial\mathcal{M}$. We next define coordinates (z, x) on the network, where z is in the radial direction and corresponds to the number MERA iterations ($z = 0$ at the boundary) and x runs along the spin chain. We will need the following two definitions to investigate the causal structure of the bulk.

Definition 4. *For a boundary region $A \subseteq \partial\mathcal{M}$ the causal past of A , $\mathcal{C}(A) \subseteq \mathcal{M}$, is defined as the set of all tensors in the network that can be reached by starting on A and tracing a path along the network edges in the direction of increasing z.*

Definition 5. *For a boundary region $A \subseteq \partial\mathcal{M}$, the past domain of the depen-dace of A, $\mathcal{D}(A)$, is defined as the set of all tensors in the network such that all paths of decreasing z intersecting the tensor must terminate on A.*

Note that the "time" related terminology here is related to the direction of the isometric flow of the network from top tensor to boundary. However in the holographic picture this is really a spacial dimension. It should be clear that for any region A, $\mathcal{D}(A)$ is contained entirely within $\mathcal{C}(A)$, and that $\mathcal{C}(A)$ always extends to the top tensor. These objects have been represented in Fig. 10. What follows are some important properties of $\mathcal{C}(A)$ and $\mathcal{D}(A)$

- The network defined by $\mathcal{C}(A)$ is always a quantum state, $\mathcal{C}(A) \in \mathcal{H}_A \otimes \mathcal{H}_{\gamma_1}$, where $\mathcal{H}_A$ is the Hilbert space corresponding to the boundary region A

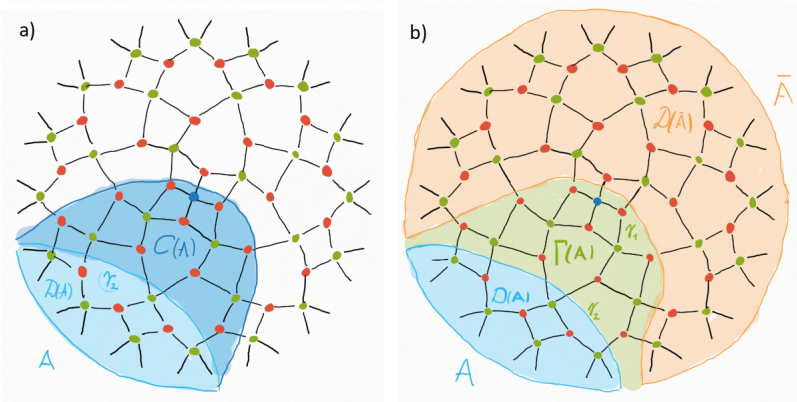

Figure 10: a) Here we have shown the domain of dependance, $\mathcal{D}(A)$ and causal past, $\mathcal{C}(A)$, for a subregion A, where the light blue region is to be understood as also part of $\mathcal{C}(A)$. b) Here the network has been equivalently decomposed into the isometries $\mathcal{D}(A)$ (blue) and $\mathcal{D}(\bar{A})$ (orange) acting on the state $\Gamma(A)$ (green).

and $\mathcal{H}_{\gamma_1}$ is the Hilbert space of the network legs that are intersected by the bulk surface γ_1, that bounds $\mathcal{C}(A)$.

- The network defined by $\mathcal{D}(A)$ is always an isometry, $\mathcal{D}(A) : \mathcal{H}_{\gamma_2} \to \mathcal{H}_A$, where $\mathcal{H}_{\gamma_2}$ is the Hilbert space of the network legs that are intersected by the bulk surface γ_2, that bounds $\mathcal{D}(A)$
- The complement of $\mathcal{D}(A)$ is always $\mathcal{C}(\bar{A})$, where $\bar{A}$ is the boundary complement of A. It follows then that $\mathcal{D}(A) \times_{\gamma_2} \mathcal{C}(\bar{A}) = \mathcal{D}(\bar{A}) \times_{\gamma_1} \mathcal{C}(A) = \mathcal{M}$, where $\times_\gamma$ is shorthand for the contraction of indices defined on surface γ.
- It will also be useful to define the state $\Gamma(A) = \mathcal{D}(A)^\dagger \times_A \mathcal{C}(A)$, with $\Gamma(A) \in \mathcal{H}_{\gamma_1} \otimes \mathcal{H}_{\gamma_2}$.
  From which it follows that $\big(\mathcal{D}(A) \otimes \mathcal{D}(\bar{A})\big) \times_{\gamma_1 \cup \gamma_2} \Gamma(A) = \mathcal{M}$.
- The minimal bulk curve (in terms of intersected legs) that shares its boundary with A is exactly the smaller of the two curves γ_1 and γ_2.

For a computational point of view $\mathcal{C}$ is of great importance. If we wish to compute the expectation value of an observable defined on a region A then we only need to consider tensors in $\mathcal{C}(A)$, which greatly reduces the number of contractions required compared to contracting the entire network. Additionally it is a feature of any MERA that for large enough z the width of $\mathcal{C}$ is upper bounded by some fixed constant that depends on the specific MERA being used. The domain of dependence however is more interesting from a holographic point of view, as it is the tensor network analog of the entanglement wedge. This is because if we make some change to any of the tensors in $\mathcal{D}(A)$ the effect can equivalently be achieved by acting on the original boundary state with a unitary that has support on A.

5.1.1 The RT like entanglement structure of MERA

With Def. 4 and Def. 5 in hand, we can now show how the entanglement entropy of MERA states satisfies a bound analogous to the RT formula of standard holography. We begin by bipartitioning the boundary of our network, $\mathcal{M}$, into a connected subregion A and it's complement $\bar{A}$. Such that the state defined by $\mathcal{M}$ is $|\mathcal{M}\rangle \in \mathcal{H}_A \otimes \mathcal{H}_{\bar{A}}$. As we outlined above we can rewrite $|\mathcal{M}\rangle$ as,

$$|\mathcal{M}\rangle = (\mathcal{D}(A) \otimes \mathcal{D}(\bar{A}))\, |\Gamma(A)\rangle\,, \tag{86}$$

where we have omitted the $\times$-notation as the implied contractions should be clear from the context.
To determine the entanglement entropy across the two regions we start, as usual, by taking the partial trace of $|\mathcal{M}\rangle$ over region $\bar{A}$.

$$\begin{aligned}
\rho_A &= \mathrm{Tr}_{\bar{A}}\left[|\mathcal{M}\rangle\langle\mathcal{M}|\right] \\
&= \mathcal{D}(A)\,\mathrm{Tr}_{\bar{A}}\left[(I\otimes\mathcal{D}(\bar{A}))\,|\Gamma(A)\rangle\langle\Gamma(A)|\,(I\otimes\mathcal{D}^\dagger(\bar{A}))\right]\mathcal{D}^\dagger(A) \\
&= \mathcal{D}(A)\,\mathrm{Tr}_{\gamma_1}\left[|\Gamma(A)\rangle\langle\Gamma(A)|\right]\mathcal{D}^\dagger(A) \\
&\equiv \mathcal{D}(A)\rho_{\gamma_2}\mathcal{D}^\dagger(A).
\end{aligned} \tag{87}$$

In the second line we have simply taken $\mathcal{D}(A)$ outside of the trace, and in the third line we have used the cyclic property of the trace and the fact that $\mathcal{D}(\bar{A}) : \mathcal{H}_{\gamma_1} \to \mathcal{H}_{\bar{A}}$. Now determining the entropy it follows, from the invariance under isometry property, that,

$$S(\rho_A) = S(\rho_{\gamma_2}). \tag{88}$$

We can determine the upper bound on $S(\rho_A)$ then by assuming that $|\Gamma(A)\rangle$ has maximal entanglement between γ_1 and γ_2, in which case,

$$\begin{aligned}
S(\rho_{\gamma_2}) &= \log\left(\min\left(\dim\mathcal{H}_{\gamma_1}, \dim\mathcal{H}_{\gamma_2}\right)\right) \\
&= \log\left(\min\left(\chi^{|\gamma_1|}, \chi^{|\gamma_2|}\right)\right) \\
&= \log(\chi)\min\left(|\gamma_1|, |\gamma_2|\right) \\
&= \log(\chi)|\gamma^*|.
\end{aligned} \tag{89}$$

In the second line we have written the Hilbert space dimension in terms of the bond dimension χ, and $|\gamma|$, the number of legs intersected by surface γ. In the last line γ^* denotes the shorter of the two surfaces. It then immediately follows that,

$$S(\rho_A) \leq \log(\chi)|\gamma^*|. \tag{90}$$

We see then, that the upper bound on the entanglement entropy of a boundary subregion, is proportional to length of the minimal bulk curve homologous to the said boundary region. Evidently this is in exact correspondance with the Ryu-Takayanagi formula. Of course there is the crucial difference that what we have here is merely an upper bound and not an exact equality, and so it will

therefore be important to ask what conditions are neccesarry for the bound to be saturated. We will return to this question in the following section when we introduce the HaPPY network and perfect tensors. Furthermore, since for a well optimized MERA $S(\rho_A)$ should be approximately the entanglement entropy of a $1+1$-dimensional CFT,

$$\frac{c}{3}\log\left(\frac{l}{a}\right) \leq |\gamma^*|\log(\chi). \tag{91}$$

And by consequce of the network structure $|\gamma^*| \approx \alpha \log\left(\frac{l}{a}\right)$, for some constant α. Therefore,

$$\begin{aligned} \frac{c}{3} &\leq \alpha \log(\chi) \\ \frac{R}{2G} &\leq \alpha \log(\chi) \end{aligned} \tag{92}$$

where in the second line we have used the identification of central charge with AdS radius from the Ryu-Takayanagi formula.

5.1.2 Defining a metric for the MERA geometry

Taking seriously the idea that entanglement entropy corresponds to area (length in 1+1D) in the bulk we can next define a metric for the emergent geometry. Considering first the coordinate that runs along the lattice, the length of an interval at constant z is given by $x = a_z n$, where a_z is the lattice spacing at RG cutoff z and n is the number of sites the curve intersects. Defining $a_0 = a$, then for a binary MERA network we have $a_z = a2^z$. Then for constant z the differential entropy is given by,

$$dS \leq \log(\chi)\frac{2^{-z}dx}{a}. \tag{93}$$

We next consider the scale coordinate z. Starting at the point (x_0, z_0) the minimal number of legs crossed to reach (x_0, z_0+1) is either 1 or 2 depending on the particular x_0, this is a consequence of the fact that the MERA network is not translation invariant. However, the distance is independent of z. Therefore for constant x we get,

$$dS \leq 2\log(\chi)dz. \tag{94}$$

We can now combine these results to obtain,

$$dS^2 \leq \log^2(\chi)\left(4dz^2 + \frac{2^{-2z}dx^2}{a^2}\right), \tag{95}$$

which after coordinate transform $r = a2^z$, simplifies to,

$$dS^2 \leq \log^2(\chi)\left(\frac{4}{\ln^2(2)}\frac{dr^2}{r^2} + \frac{dx^2}{r^2}\right). \tag{96}$$

Comparing this with the induced metric on a time slice of AdS3, we can immediately see the similarity,

$$ds^2 = R^2 \left(\frac{dr^2}{r^2} + \frac{dx^2}{r^2} \right). \tag{97}$$

Firstly, it is evident we must identify R with $\log(\chi)$, and as (92) suggest this is a reasonable identification. Secondly, we see that the main discrepancy arises from the multiplicative factor $\backsim 10$ in front of the dr^2 term, this discrepancy is consequence of the lack of translation symmetry as mentioned earlier, but also the fact that our RG scheme is discrete as opposed to continuous. However, this discrepancy can be tamed slightly by noting that the bulk legs that are traversed when moving in the radial direction are often the outgoing legs of the isometries, which will, as a consequence of the nature of the disentanglers, have lower entropy than other legs. This reduction in entropy in the radial direction will somewhat suppress the larger multiplicative factor on the dr^2 term in the metric.

Furthermore since we are equating the length of a curve with the total entropy of legs intersected, what we actually have is a measure of distance between the tiles of the network, which have the legs as their edges and tensors as their vertices. In other words the metric is in fact defined on the dual network and not the tensor network itself, see Fig. 11b.

5.1.3 Some problems

So far we have seen that MERA shows some promising similarities with AdS/CFT. We have an upper bound on entanglement entropy of boundary subregions that has the same form as the RT formula, and we have defined a metric for the bulk that has a hyperbolic geometry similar to spatial slices of anti-de Sitter spacetimes. However the analogy is clearly not perfect. The most obvious issue is that in both cases we have an upper bound and not an equality. However, another issue with the interpretation is the behaviour of entanglement wedges. As discussed, for any bipartition of the boundary the network correspondingly decomposes according to (86). The issue is that there is a large bulk region, corresponding to $|\Gamma\rangle$, which does not belong in either the entanglement wedge of A or the entanglement wedge of $\bar{A}$. This is an issue because in true holography we would expect the entanglement wedges of complementary regions on the boundary to form complementary regions in the bulk[5].

Both of these issues can in fact be traced back to the fact that MERA networks are inherently anisotropic. First of all the existence of the top tensor in effect selects a prefered centre in the bulk, in true AdS/CFT the centre at $r = 0$ is simply a feature of the coordinante system where as in MERA this is a genuine feature of the network geometry. The second source of this anisotropy is the fact that the tensors in the network only act as isometries in the radial

[5]More precisely for a bulk Cauchy slice, Σ_B, that contains the extremal surface and asymptotes to the boundary slice of interest, $\Sigma_b = A \cup \bar{A}$, then $(\mathcal{W}(A) \cap \Sigma_B) \cup (\mathcal{W}(\bar{A}) \cap \Sigma_B) = \Sigma_B$

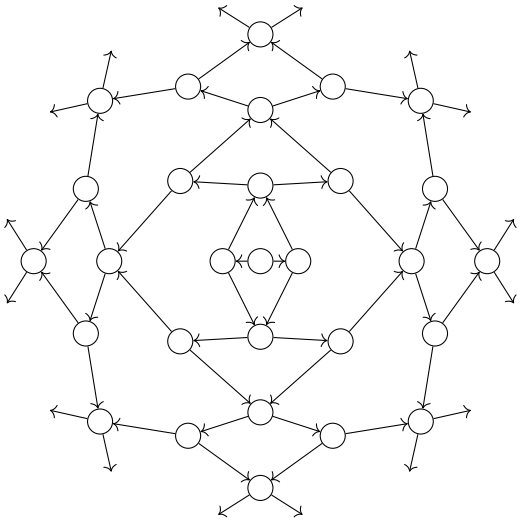

(a)

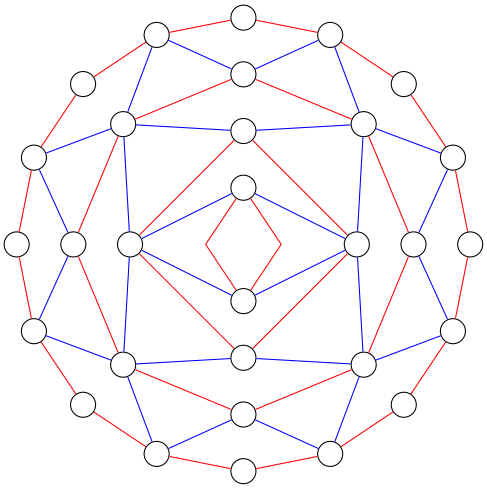

(b)

Figure 11: Here we have shown a MERA network with peridoic boundary conditions, (a), and it's dual network, (b), where the nodes in the dual network correspond to the tiles bounded by the legs of the original network. The red edges correspond to crossing the outgoing legs of disentanglers and the blue edges correspond to crossing the outgoing legs of isometries, and we can therefore expect the distance along blue legs to be shorter.

direction. As we will see in the next section HaPPY networks have neither of these anisotropic qualities and as a result resolve both of the issues discussed.

5.2 HaPPY networks: perfect tensors & error correction

HaPPY networks, named for the initials of the original authors [12], were devised as a simple tensor network toy-model of holography, that would exhibit the quantum error correcting properties expected of the bulk to boundary map in AdS/CFT [10]. As a consequence of its construction it satisfies an RT formula for the entanglement entropy, but as opposed to MERA this is an equality and not an upper bound. HaPPY networks are also well suited to not only build holographic states but build an isometric mapping from a subspace of the bulk Hilbert space to the Hilbert space of the boundary. The resulting mapping then exhibits behaviour similar to entanglement wedge reconstruction. We will now introduce the key ingredient to HaPPY networks before outlining the full construction.

5.2.1 Perfect tensors

As we discussed earlier one of the issues with holographic MERA is that the tensors in the network only act as isometries in the radial direction, so if we could restrict to tensors that act as isometries in any direct, i.e. for any bipartition of its legs, then this issue would be resolved. It is exactly this quality that makes perfect tensors, so called "perfect".

Definition 6. *A perfect tensor, T, is a tensor of even order which for any bipartition of its indices is proportional to an isometry from the smaller set of indices to the larger set of indices.*

Perfect tensors are actually based on a similar idea put forward by the quantum information theory community a few years prior. With the goal of finding classes of quantum states that would allow for improved versions of quantum teleportation [64], absolutely maximally entangled (AME) states were introduced [65]. These are multipartite states for which there is maximal entanglement for any bipartition of the state. Under the Choi–Jamiołkowski isomorphism Eq. (22) theses states are then in one-to-one correspondence with perfect tensors. A sufficient condition for a tensor to be perfect, is that for every bipartition of the indices, such that both sets are equal in size, the tensor acts as a unitary between the two sets of indices.

5.2.2 Construction of the network

The other issue with holographic MERA was that the existence of the top tensor induces a preferred centre. HaPPY networks avoid this issue by using a network structure that has a higher degree of symmetry. Namely, the network structure is informed by some uniform tiling of the hyperbolic plane (equal time slice of AdS3). A perfect tensor is then placed on each tile and legs are

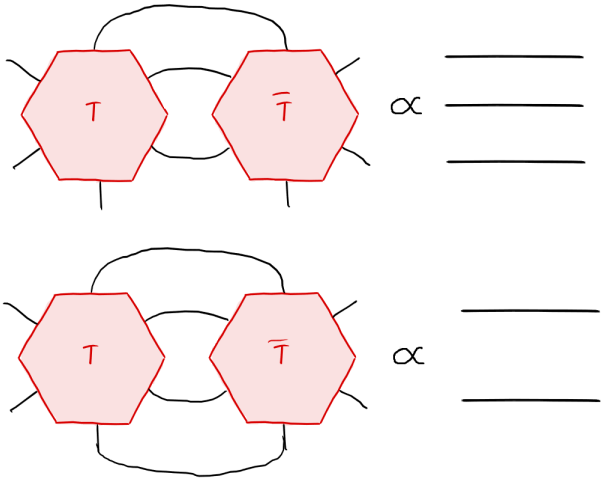

Figure 12: Examples of two possible contractions of the perfect tensor, T, with its conjugate are shown. In both cases the result is proportional to the identity, showing that T is indeed proportional to an isometry for both partitions. Furthermore interpreting T as a state then the figures correspond to partial traces resulting in reduced density matrices proportional to the identity, and so T is indeed an AME state.

contracted between tensors whose tiles share an edge. By construction this network will be invariant under a change of centre due to the isomorphisms of the tiling. Obviously, any such tiling of hyperbolic space necessarily has an infinite number of tiles. Practically however, we cannot deal with an infinite tensor network so the network is terminated after a certain amount of layers. This can be understood as analogous to an RG cutoff, it's worth noting that this cutoff will break this centre invariance we just invoked. However, HaPPY networks restore this invariance in the infinite limit, whereas MERA necessarily has a centre even in the infinite limit.

To give an example of this general construction, we can inscribe a hexagonal tiling on the hyperbolic plane and then place a six-legged perfect tensor on each tile, as shown in Fig. 13. Such a network will then produce (up to normalization) a state at the boundary, $|\Psi_b\rangle$. With the network constructed lets now inspect some of it's holographic properties

5.2.3 Ryu-Takayanagi in HaPPY states

In calculating the entanglement entropy of a subregion in MERA we were able to use concepts like the causal past and domain of dependence in the network. However these concepts are a consequence of the directionality of MERA, and since we have done away with this in HaPPY, we will require a different ap-

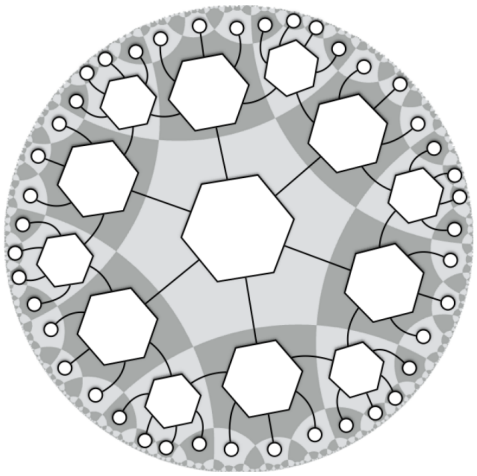

Figure 13: Here we have a HaPPY network based on a hexagonal tiling. Figure taken from [12].

proach. The approach will similarly take advantage of the fact that the entanglement entropy between two regions is invariant under local isometries.

As usual we bipartition the boundary legs into two regions A and $\bar{A}$. We then select a tensor that has at least half of its legs uncontracted and in A. We then contract the legs in A with the conjugate tensor. Because of the perfect propert this produces the identity, and so we have effectively removed the tensor from the network. This results in a new boundary subregion A' for which $\partial A' = \partial A$ but now extends into the bulk, including the legs that have now become uncontracted by the removal of the tensor. We then search for a new tensor to remove, the critera now being that it has at least half of its legs uncontracted and in A'. Again we contract with its conjugate to remove the tensor. We continue this process until no more tensors can be removed in this manner. The resulting surface is labelled γ_A, and is exactly the minimal bulk surface homologous to A. See Fig. 14

We can now apply the same process to the subregion, $\bar{A}$, and we will find that the resulting minimal surface is exactly that obtained from starting on A. What this is telling us is that the HaPPY network can be decomposed according to,

$$
\begin{aligned}
|\Psi_b\rangle &= \left(\mathcal{D}(A)\otimes\mathcal{D}(\bar{A})\right)\left(\bigotimes_{j=1}^{|\gamma_A|}\left|\Phi_j^+\right\rangle\right), \\
\left|\Phi_j^+\right\rangle &= \frac{1}{\sqrt{\chi}}\sum_{i=1}^{\chi}|i\rangle_{\gamma_j}\otimes|i\rangle_{\bar{\gamma}_j}\in\mathcal{H}_{\gamma_j}\otimes\mathcal{H}_{\bar{\gamma}_j}, \\
\mathcal{D}(A) &: \bigotimes_j \mathcal{H}_{\gamma_j}\to\mathcal{H}_A,\ \mathcal{D}(\bar{A}) : \bigotimes_j \mathcal{H}_{\bar{\gamma}_j}\to\mathcal{H}_{\bar{A}},
\end{aligned}
\tag{98}
$$

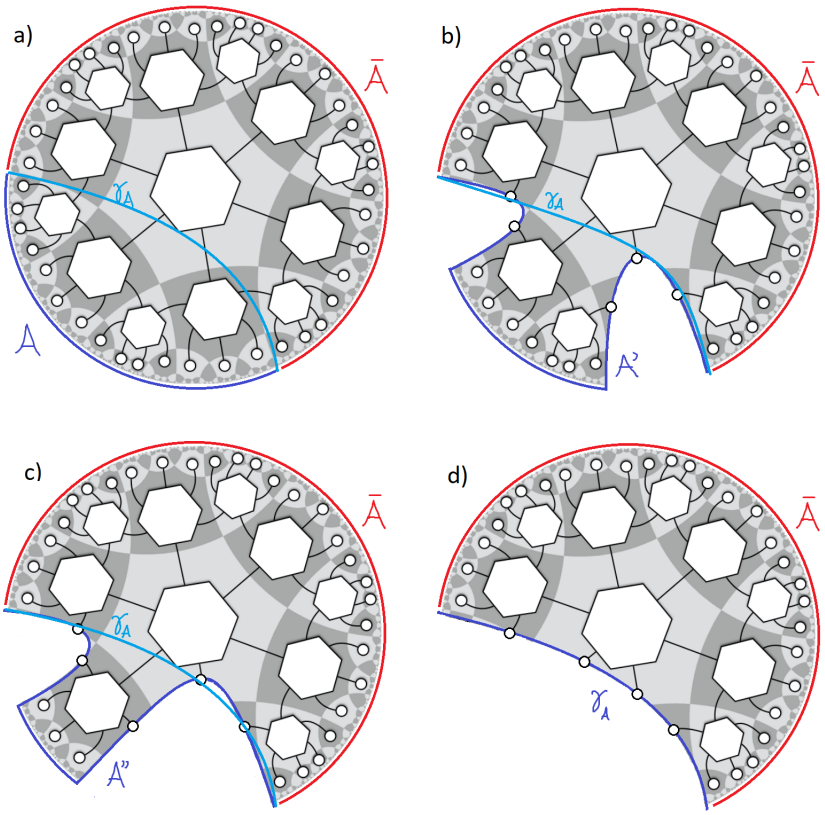

Figure 14: We show here various intermidiate steps in obtaining the RT surface. a) Shows the partiton of the boundary into A and $\bar{A}$ and the minimal surface, γ_A, already inscribed for clarity. b) - c) Show intermidiate steps in the process, where some tensors have been removed as we describe and the new surfaces A' and A'' have been marked in blue. d) The point has been reached where tensors can no longer be removed from the A side and we see that the resulting surface corresponds exactly to γ_A. The same process is then applied to $\bar{A}$.

where the $\mathcal{D}(A)$ and $\mathcal{D}(\bar{A})$ isometries are formed from the composition of the tensors we removed from the A and $\bar{A}$ side respectively. The appearance of the maximally entangled states is a consequence of the fact that all tensors in the network have been absored into either A or $\bar{A}$ so all that is left is the factors of the identity that connect $\mathcal{D}(A)$ to $\mathcal{D}(\bar{A})$. However under the Choi–Jamiołkowski isomorphism the identity is equivalent to a maximmally entangled state. Therefore by the invariance of entropy under isometries we know that the entanglement entropy of A is exactly the entanglement entropy of the maximally entangled states defined on γ_A, and so,

$$S(A) = |\gamma_A| \log(\chi). \tag{99}$$

Therefore we have shown that HaPPY states indeed satisfy a Ryu-Takayanagi equation for the entanglement entropy. Furthermore in comparison to MERA, where for a bipartition of the boundary we could decompose the bulk according to Eq.(86), where a large region of the bulk is unaccounted for by either entanglement wedge. Here we have that the union of the complementary wedges is the entire bulk as we would expect in true AdS/CFT.

5.2.4 HaPPY codes: bulk to boundary maps

In the original paper [12], these HaPPY networks were used not just to build a single boundary state but also to construct isometric maps from the bulk Hilbert space to the boundary Hilbert space, in such a manner that the quantum error correcting properties of holography are exhibited. To build these HaPPY codes, we must leave some legs uncontracted, not just on the boundary but also in the bulk. The resulting tensor network is understood not as a state on all the uncontracted legs but as a map from the bulk legs to the boundary legs. We will now outline the construction of such a map.

For brevity we shall construct the map using the same six-legged perfect tensors as before. The difference being that we now use a pentagonal tiling of the hyperboic plane and as before place a tensor on each tile, contracting between neighbouring tiles. As a result we will now have a free leg in the bulk for each tensor in the network, see Fig. 15 These legs are then understood as the bulk Hilbert space, $\mathcal{H}_B$. We then have that the network defines an isometry,

$$\mathcal{M} : \mathcal{H}_B \to \mathcal{H}_b, \tag{100}$$

such that for a certain bulk state, $|\Psi_B\rangle$, a boundary state can be obtain,

$$|\Psi_b\rangle = \mathcal{M} |\Psi_B\rangle . \tag{101}$$

Furthermore, the Ryu-Takayanagi formula satisfied by the HaPPY state construction now generalises to a QES formula. This can be readily seen if we again decompose the network into the two subnetworks defined by the minimal surface for some bipartition of the boundary. Whereas before the subnetworks defined isometries from the surface state to the boundary, we now have the isometies,

$$\begin{aligned} \mathcal{D}(A) &: \mathcal{H}_\gamma \otimes \mathcal{H}_\mathcal{W} \to \mathcal{H}_A, \\ \mathcal{D}(\bar{A}) &: \mathcal{H}_{\bar{\gamma}} \otimes \mathcal{H}_{\bar{\mathcal{W}}} \to \mathcal{H}_{\bar{A}}, \end{aligned} \tag{102}$$

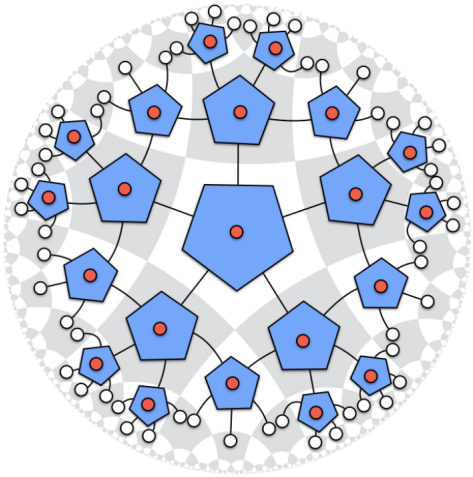

Figure 15: Here we have the HaPPY map, the red dots are understood to be the free bulk legs. Figure taken from [12]

where $\mathcal{H}_{\mathcal{W}}$ is the Hilbert space of the bulk legs in the entanglement wedge of A and similarly for $\bar{A}$. The full bulk Hilbert space is then, $\mathcal{H}_B = \mathcal{H}_{\mathcal{W}} \otimes \mathcal{H}_{\bar{\mathcal{W}}}$. It follows then that we can equivalently write the boundary state as,

$$|\Psi_b\rangle = (\mathcal{D}(A) \otimes \mathcal{D}(\bar{A})) \left(|\Phi\rangle_{\gamma\bar{\gamma}} \otimes |\Psi_B\rangle_{\mathcal{W}\bar{\mathcal{W}}} \right), \tag{103}$$

where $|\Phi\rangle$ is understood to be the collection of maximally entangled states that straddle the minimal surface. The reduced density matrix on A is then given by,

$$\rho_A = \mathcal{D}(A) \left(\mathrm{Tr}_{\bar{\gamma}} \left[|\Phi\rangle \langle\Phi| \right] \otimes \mathrm{Tr}_{\bar{\mathcal{W}}} \left[|\Psi_B\rangle \langle\Psi_B| \right] \right) \mathcal{D}^\dagger(A), \tag{104}$$

from which it follows the entanglement entropy of A is,

$$S(A) = |\gamma_A| \log(\chi) + S(\mathcal{W}), \tag{105}$$

where $S(\mathcal{W})$ is the entanglement entropy of the bulk state between the two wedges.

It is clear that in these HaPPY codes the bulk Hilbert space will always be of smaller dimension than the boundary Hilbert space. We therefore are only able to map bulk states to a subspace of the boundary Hilbert space, namely the image of the HaPPY code. This may seem a disadvantage of the map but in fact it is a key feature. It is exactly this quality that allows for the quantum error correcting properties of the network, properties that are now understood to be cruicial to understanding the AdS/CFT correspondence [10]. Indeed locality in the bulk can only be satisfied within certain code subspaces of the theory. Furthermore by the fact that a local bulk operator can exist in the entanglement wedge of many different regions simultaneously, this implies

there are many different boundary operators that correspond to the same bulk operator. This redundancy of the boundary representation would be paradoxical if we did not restrict the bulk to a code subspace. Even the ability to equate boundary entropy with a bulk area is a consequence of the code subspace and in fact a property that is present in many QECCs even outside of holography [66].

5.2.5 Some problems

It seems that HaPPY has overcome all of the issues MERA has when interpreted holographically. We have shown that the Ryu-Takayanagi formula is satisfied exactly, and that the entanglement wedges of complementary regions cover the untire bulk. Furthermore, they easily generalize to maps from the bulk to the boundary, satisfying now a QES like equation and exhibiting quantum error correcting properties. However, these nice qualities have not come for free, and in fact the price ultimately means that we cannot directly use HaPPY networks in our goal of simulating bulk dynamics.

First of all, as we have shown, when computing the entanglement entropy of a subregion the network can be restructured as a pair of isometries acting on a collection of maximally entangled states. It is exactly this property that causes the RT bound to be saturated. However, this also means that the entanglement spectrum for any region is completely flat, meaning all the reduced density matrix eigenvalues are the same or equivalently all Renyi entropies are the same. Any quantum system that has a true holographic dual cannot possibly have such simple entanglement structure [67]. The second problem, and the more damning of the two for our purposes, is that HaPPY networks do not form a suitable ansatz for any known physical system, least of all CFTs. Already from the first issue we know they are not capable of reproducing the entanglement structure of CFT states, but more importantly we are not capable of associating a boundary Hamiltonian with the network, as we do in MERA. If we could somehow define a suitable boundary Hamiltonian then one can imagine using the HaPPY code to map this to a bulk Hamiltonian and from there simulate the bulk dynamics. It seems then that we have two different ends of the spectrum here. On one hand we have a network that accurately approximates ground states of CFTs while also crudely exhibiting holographic properties, and on the other hand we have a network that satisfies very clean and exact holographic properties but does not have a real physical system associated with it. Our goal then in the next section and the ultimate goal of this thesis, is to find a compromise between these two extremes.

6 Tackling the dynamics problem

We now turn to the problem of trying to simulate bulk dynamics using holographic tensor networks. The idea of simulating real time evolution in tensor networks is not a new one, and in fact efficient algorithms for MPS states, known

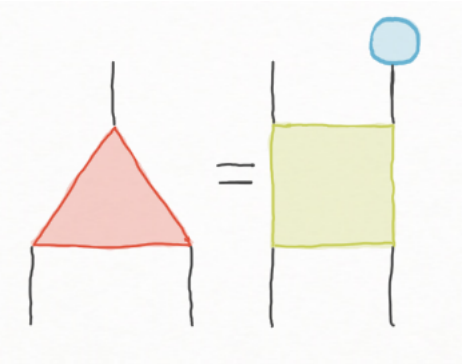

Figure 16: Here we have represented an isometry (red) as a unitary (green) with a state (blue) contracted on one leg

as time-evolving block decimation (TEBD) have existed for two decades [68]. Further still, an algorithm for time evolution of MERA was developed a few years later [69]. However, these algorithms were designed for the purposes of a condensed matter physicist, where only the output state is of interest. They pay no heed to what is happening in the bulk. As we will see, there are a few barriers to developing a concise interpretation of the bulk in a dynamical context. We will explore in this section two possible ways of interpreting bulk dynamics in tensor networks and discuss the strengths and weaknesses of both attempts.

6.1 MERA as a bulk to boundary map

As we saw in the previous section HaPPY codes provide a very clear interpretation of what is happening in the bulk. Within a certain subspace of the boundary theory we have a precise map between bulk states and boundary states. However, we cannot simulate dynamics as there is no Hamiltonian associated to the system. A possible resolution to this is to modify MERA, which can be assigned a Hamiltonian, such that it too forms a bulk to boundary map. The key to this construction is the realization that any isometry can in fact be represented as a unitary with a quantum state contracted with one of its legs. This is straight forward to show. For some unitary, $U : \mathcal{H}_A \otimes \mathcal{H}_B \to \mathcal{H}_A \otimes \mathcal{H}_B$ and state $|\psi\rangle \in \mathcal{H}_A$, we can construct an isometry as follows,

$$\begin{aligned} &W = U\left(|\psi\rangle \otimes I_B\right), \\ &W : \mathcal{H}_B \to \mathcal{H}_A \otimes \mathcal{H}_B. \end{aligned} \tag{106}$$

See Fig. 16 for the graphical representation. To show that W is indeed an

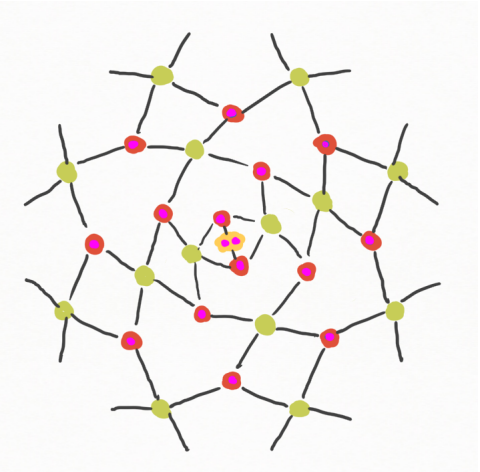

Figure 17: Here we have a MERA map network with a periodic boundary. Each tensor in the network is unitary and the purple dots represent free legs pointing out of the page, these form the bulk Hilbert space.

isometry we simply contract with its conjugate,

$$\begin{aligned} W^\dagger W &= \left(\langle\psi| \otimes I_B\right) U^\dagger U \left(|\psi\rangle \otimes I_B\right), \\ &= \langle\psi|\psi\rangle \, I_B, \\ &= I_B. \end{aligned} \tag{107}$$

For some choice of $|\psi\rangle$ we can construct any isometry $W : \mathcal{H}_B \to \mathcal{H}_A \otimes \mathcal{H}_B$ with an appropriate choice of U.

Using this idea, we can then replace every isometry in the original MERA with a unitary where the extra leg has some state contracted with it. If we also replace the two legged top tensor, which is a quantum state, with a 2 to 2 unitary then every tensor in the network is now a unitary and so we can reinterpret the network as a unitary mapping from the bulk Hilbert space to the boundary Hilbert space, where we interpret the states contracted with the extra legs of the top tensor and isometries as forming the bulk state. Therefore, by the unitarity of the network we can now, for a particular MERA network, assign a bulk state to every boundary state. Denoting this unitary network (without the contraction with bulk states) as $\mathcal{M}$, then

$$\begin{aligned} \mathcal{M} &: \mathcal{H}_B \to \mathcal{H}_b, \\ \mathcal{M}^\dagger \mathcal{M} &= \mathcal{M}\mathcal{M}^\dagger = I. \end{aligned} \tag{108}$$

where $\mathcal{H}_B$ and $\mathcal{H}_b$ are the bulk and boundary Hilbert spaces respectively. Such a network can be seen in Fig. 17. It should be clear, that the original MERA is in fact a special case of the MERA map where the bulk state is fully seperable, i.e. has no entanglement. We will now briefly discuss what this modification

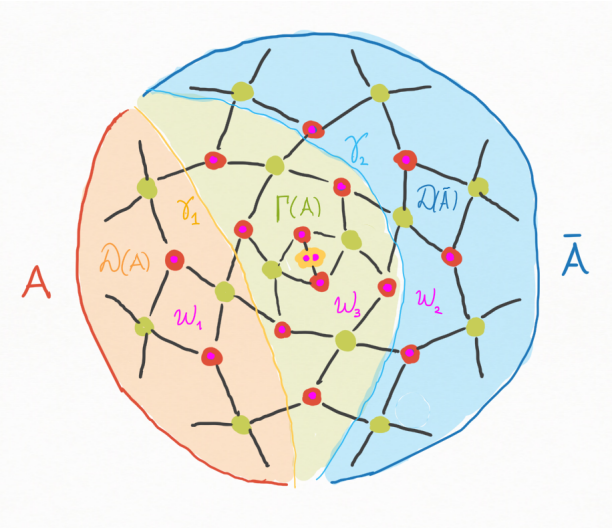

Figure 18: The MERA map is decomposed according to the boundary bipartition A and $\bar{A}$. The green subnetwork, $\Gamma(A)$, maps the $\mathcal{W}_3$ bulk subregion to the surfaces γ_1 and γ_2. The red and blue subnetworks, $\mathcal{D}(A)$ and $\mathcal{D}(\bar{A})$, map $\mathcal{W}_1$ and γ_1 to A, and $\mathcal{W}_2$ and γ_2 to $\bar{A}$ respectively.

has done to our RT bound of the original MERA, and then move on to discuss using this network to simulate dynamics.

6.1.1 Entanglement entropy in the MERA map

For a particular bipartition of the boundary A and $\bar{A}$, we decompose the network, as with the oringal MERA, into $\Gamma(A)$, $\mathcal{D}(A)$ and $\mathcal{D}(\bar{A})$. However, these subnetworks now have different roles. They now all form unitary subnetworks. Namely,

$$\begin{aligned} \Gamma(A) &: \mathcal{H}_{\mathcal{W}_3} \to \mathcal{H}_{\gamma_1} \otimes \mathcal{H}_{\gamma_2}, \\ \mathcal{D}(A) &: \mathcal{H}_{\mathcal{W}_1} \otimes \mathcal{H}_{\gamma_1} \to \mathcal{H}_A, \\ \mathcal{D}(\bar{A}) &: \mathcal{H}_{\mathcal{W}_2} \otimes \mathcal{H}_{\gamma_2} \to \mathcal{H}_{\bar{A}}, \end{aligned} \tag{109}$$

where $\mathcal{H}_{\mathcal{W}_1}$, $\mathcal{H}_{\mathcal{W}_2}$ and $\mathcal{H}_{\mathcal{W}_3}$ are the Hilbert spaces of the bulk legs attached to $\mathcal{D}(A)$, $\mathcal{D}(\bar{A})$ and $\Gamma(A)$ respectively, and so $\mathcal{H}_{\mathcal{W}_1} \otimes \mathcal{H}_{\mathcal{W}_2} \otimes \mathcal{H}_{\mathcal{W}_3} = \mathcal{H}_B$. As before, $\mathcal{H}_{\gamma_1}$ and $\mathcal{H}_{\gamma_2}$ are to be understood as the Hilbert spaces of the contracted legs that connect $\Gamma(A)$ to $\mathcal{D}(A)$ and $\mathcal{D}(\bar{A})$ respectively. These subnetworks and associated Hilbert spaces are all represented in Fig. 18. It will also be useful to note that,

$$\begin{aligned} \mathcal{D}(A) \times_{\gamma_1} \Gamma(A) = \mathcal{C}(A) &: \mathcal{H}_{\bar{\mathcal{W}}_2} \to \mathcal{H}_A \otimes \mathcal{H}_{\gamma_2}, \\ \mathcal{D}(\bar{A}) \times_{\gamma_2} \Gamma(A) = \mathcal{C}(\bar{A}) &: \mathcal{H}_{\bar{\mathcal{W}}_1} \to \mathcal{H}_{\bar{A}} \otimes \mathcal{H}_{\gamma_1}, \end{aligned} \tag{110}$$

where both $\mathcal{C}$'s also form unitary subnetworks, and $\mathcal{H}_{\bar{\mathcal{W}}_1}$ and $\mathcal{H}_{\bar{\mathcal{W}}_2}$ are shorthand for $\mathcal{H}_{\mathcal{W}_2} \otimes \mathcal{H}_{\mathcal{W}_3}$ and $\mathcal{H}_{\mathcal{W}_1} \otimes \mathcal{H}_{\mathcal{W}_3}$ respectively. For a particular bulk state, $|\Psi_B\rangle \in \mathcal{H}_B$, we then obtain the boundary state by,

$$\begin{aligned} |\Psi_b\rangle &= \left(I_A \otimes \mathcal{D}(\bar{A})\right)\left(I_{\mathcal{W}_2} \otimes \mathcal{C}(A)\right)|\Psi_B\rangle\,, \\ &= \left(I_{\bar{A}} \otimes \mathcal{D}(A)\right)\left(I_{\mathcal{W}_1} \otimes \mathcal{C}(\bar{A})\right)|\Psi_B\rangle\,. \end{aligned} \tag{111}$$

In obtaining our modified RT bound it will be useful to calculate both ρ_A and $\rho_{\bar{A}}$, which by purity of the bulk state will have the same entropy. Starting with ρ_A we get,

$$\begin{aligned} \rho_A &= \mathrm{Tr}_{\bar{A}}\left[\left(I_A \otimes \mathcal{D}(\bar{A})\right)\left(I_{\mathcal{W}_2} \otimes \mathcal{C}(A)\right)|\Psi_B\rangle\langle\Psi_B|\left(I_{\mathcal{W}_2} \otimes \mathcal{C}(A)^\dagger\right)\left(I_A \otimes \mathcal{D}(\bar{A})^\dagger\right)\right], \\ &= \mathrm{Tr}_{\gamma_2\mathcal{W}_2}\left[\left(I_{\mathcal{W}_2} \otimes \mathcal{C}(A)\right)|\Psi_B\rangle\langle\Psi_B|\left(I_{\mathcal{W}_2} \otimes \mathcal{C}(A)^\dagger\right)\right], \\ &= \mathrm{Tr}_{\gamma_2\mathcal{W}_2}\left[|\Phi_A\rangle\langle\Phi_A|\right], \end{aligned} \tag{112}$$

in the second line we used the cyclic property of the trace and in the second line we define $\left(I_{\mathcal{W}_2} \otimes \mathcal{C}(A)\right)|\Psi_B\rangle = |\Phi_A\rangle \in \mathcal{H}_{A\gamma_2\mathcal{W}_2}$. Similarly for $\rho_{\bar{A}}$ we get,

$$\rho_{\bar{A}} = \mathrm{Tr}_{\gamma_1\mathcal{W}_1}\left[|\Phi_{\bar{A}}\rangle\langle\Phi_{\bar{A}}|\right], \tag{113}$$

where $\left(I_{\mathcal{W}_1} \otimes \mathcal{C}(\bar{A})\right)|\Psi_B\rangle = |\Phi_{\bar{A}}\rangle \in \mathcal{H}_{\bar{A}\gamma_1\mathcal{W}_1}$. We can now use the strong subadditivity of the von Neumann entropy to form our RT bound,

$$S(A\gamma_2\mathcal{W}_2) + S(A) \leq S(A\gamma_2) + S(A\mathcal{W}_2),$$

we are using a shorthand here where, for example, $S(A\gamma_2)$ denotes the entropy of the reduced density matrix of $|\Phi\rangle_A$ on $\mathcal{H}_A \otimes \mathcal{H}_{\gamma_2}$. Now, by purity of $|\Phi_A\rangle$ it follows that,

$$\begin{aligned} S(A\gamma_2\mathcal{W}_2) &= 0, \\ S(A\gamma_2) &= S(\mathcal{W}_2), \\ S(A\mathcal{W}_2) &= S(\gamma_2). \end{aligned}$$

Therefore strong subadditvity tells us that,

$$S(A) \leq S(\gamma_2) + S(\mathcal{W}_2) \leq |\gamma_2|\log(\chi) + S(\mathcal{W}_2), \tag{114}$$

where the second inequality follows from the maximal value of $S(\gamma_2)$. Similarly for $|\Phi_{\bar{A}}\rangle$, we get,

$$S(\bar{A}) \leq |\gamma_1|\log(\chi) + S(\mathcal{W}_1). \tag{115}$$

However, we know that $S(A)$ and $S(\bar{A})$ must be equal so we arrive at,

$$S(A) \leq \min\left(|\gamma_1|\log(\chi) + S(\mathcal{W}_1), |\gamma_2|\log(\chi) + S(\mathcal{W}_2)\right). \tag{116}$$

It is clear to see then that the RT-like bound on entanglement entropy from the original MERA has now generalized to a QES-like bound in the MERA map.

Furthermore, it is possible to carefully select the bulk state such that the QES formula is saturated. Namely, if a state satisfies,

$$\mathrm{Tr}_{\gamma_{max}}\left[\Gamma(A)\rho_{\mathcal{W}_3}\Gamma(A)^\dagger\right] \propto I, \tag{117}$$

where $\rho_{\mathcal{W}_3}$ is the bulk reduced density matrix on $\mathcal{W}_3$ and γ_{max} is the larger of the two γ curves, then the QES formula will be saturated. We can understand such states as being somewhat analagous to the fixed-area states of [70]. Note that such a state is only guaranteed to saturate the bound for the bipartition A and $\bar{A}$.

6.1.2 Bulk dynamics with the MERA map

As we mentioned above, the MERA map when the bulk state is fully separable is equivalent to the original MERA tensor network. Without loss of generality we can then choose our inital bulk state to be, $|0\rangle^{\otimes n}$. Then for the boundary Hamiltonian we are intereseted in, we can apply the usual variational algorithms of [63] to approximate the ground state of our Hamiltonian. The end product will then be a unitary map that, to a good approximation, maps the bulk state, $|0\rangle^{\otimes n}$, to the ground state of the boundary Hamiltonian. We can then associate, $|0\rangle^{\otimes n}$, with the bulk vacuum. Since we chose the bulk state ourselves this may seem like circular logic, however it really just amounts to a choice of basis on the Hilbert space of each bulk leg. For example we could equivalently have started with the bulk state, $\bigotimes_{i=1}^{n}|\psi_i\rangle$, but under a local change of basis this state can be brought to $|0\rangle^{\otimes n}$. Note however, that this assignment does assume that the bulk vacuum state has negligible entanglement, we will return to discussing the validity of this assumption shortly.

The optimist might assume that we have already achieved our goal. We have a bulk to boundary map for some critical system, that provides a hyperbolic emergent geometry and exhibits at least approximately some of the entanglement properties of holographic systems. Using the map we can send the boundary Hamiltonian to a bulk Hamiltonian and from there simulate the bulk dynamics. However, there is an issue hiding in the details. The problem is that our choice of the unitaries that replaced the isometries of the original MERA is underconstrained. To show this we assume that W can be equivalently represented as,

$$\begin{aligned} W &= U(|0\rangle \otimes I), \\ &= V(|0\rangle \otimes I), \end{aligned} \tag{118}$$

where U and V are unitary. V can then be written in terms of U as, $V = UT$, for some unitary T. Substituting we get,

$$\begin{aligned} U(|0\rangle \otimes I) &= UT(|0\rangle \otimes I), \\ \implies (|0\rangle \otimes I) &= T(|0\rangle \otimes I). \end{aligned} \tag{119}$$

It is then straight forward to show that any T of the form,

$$T = I_{\mathcal{H}_0} \oplus \tilde{T}_{\mathcal{H}_\perp}, \tag{120}$$

satisfies this equation, where $\mathcal{H}_0 = \text{span}\{|0\rangle \otimes |j\rangle\, |\forall j\}$ and $\tilde{T}_{\mathcal{H}_\perp}$ is a unitary acting on $\mathcal{H}_\perp$, the orthogonal complement of $\mathcal{H}_0$. Therefore the U's we obtain from the optimization algorithm, can be replaced with any unitary $V = UT$, with T satisfying Eq. (120), and we will still have a bulk to boundary map that sends $|0\rangle^{\otimes n}$ to the ground state. Crucially however, these networks will act very differently on the rest of our Hilbert space. Therefore the bulk Hamiltonian we obtain by the map is not unique. This redundancy could be interpreted as a fundamental flaw in our construction or more optimistically a gauge symmetry of the bulk theory, perhaps somehow reflecting diffeomorphism invariance. Either way if we wish obtain a clear interpretation of the bulk we need a way to make a canonical choice of T for each isometry, or in other words fix the gauge. Unfortunately we have not been able to find a sensible way of doing this.

In [20], MERA was similarly used as a bulk to boundary map. The approach used here to choose the tensors in the network is indeed constraining enough that there is no redundancy in the choice of tensors. However this method is dependent on first obtaining the boundary ground state exactly by diagonalization. Obviously then this approach is not scalable and somewhat defeats the purpose of tensor networks.

6.1.3 Closing remarks

Clearly this approach could be quite promising provided we can somehow fix the gauge in the bulk theory. Let's assume for a moment that this has been achieved so that we can explore some features of such a map.

Bulk entanglement: N, χ and G_N

In the construction of the map we assumed that the bulk vacuum state could be assumed to have negligible entanglement. This seems like an unusual assumption. However, as we know from our study of extremal surfaces in holography, the leading term in the expression for entanglement entropy at large N is given by the area of the extremal surface, this is an $\mathcal{O}(N^2)$ contribution. The contribution of the bulk entanglement is only a $\mathcal{O}(N^0)$ correction. Therefore we can expect that the fully separable bulk vacuum is a good approximation for large N theories. Somewhat analogously, we know that in the original MERA, the larger the bond dimension χ the better the approximation of the ground state. Since we know that the original MERA is equivalent to the MERA map with a fully separable bulk state, then it follows that large χ MERA maps are able to better approximate the boundary ground state with a fully separable bulk state. In this sense the large χ limit behaves similarly to the large N limit. Furthermore we know that $G_N \sim \frac{1}{N^2}$ and in all our RT formulas $\log(\chi)$ has played the role of $\frac{1}{4G_N}$, so we can loosely say $\log(\chi) \sim N^2$. If we also consider the fact that increasing χ requires some transitional layers that increase the local Hilbert space dimension this identification seems even more plausible. Essentially large χ networks can be understood as geometrizing more of the entanglement of the boundary, while networks with smaller χ geometrize some

of the entanglement while leaving some to be interpreted as the entanglement of bulk fields. In this sense there doesn't seem to be a clear prescription for which part of the entanglement structure is geometric in nature and which isn't.

Bulk locality

We lastly comment on whether we can expect the bulk Hamiltonian that we obtain to be local. In fact, it is unfortunately the case that in general we will obtain a highly non local Hamiltonian. For example if our boundary Hamiltonian is composed of 2-local terms, e.g. $\sigma_x \otimes \sigma_x + I \otimes \sigma_z$ in the critical Ising model, then the corresponding term in the bulk will have support on the entire bulk region defined by $\mathcal{C}(h)$. Where h is the 2 site boundary region that the local term is supported on. We will then obtain for every local boundary term, an operator that extends from the boundary all the way to the top tensor with a width upper bounded by 3-bulk sites (in binary MERA). We can maybe hope that in the summation of these terms the non-locality will cancel out but there is no guarantee of this being the case. In [20] they found some evidence that locality in the bulk is imposed dynamically, but their analysis was for an Ising model boundary theory that is far from the critical point so whether the holographic interpretation is valid is unclear. It is also possibility, that for a particular boundary Hamiltonian there is a choice of T in our isometry to unitary transformation that suppresses the nonlocal behaviour. However, even if said T exists there is no clear way in which it could be determined.

6.2 Bulk dynamics from bond matrices

The second attempt at obtaining bulk dynamics from MERA will be built on the original MERA network, i.e. no bulk legs. The prespective here will be to interpret the manner in which the tensors themselves evolve in time as encoding the bulk dynamics, as opposed to the previous attempt where the tensors are held fixed. We will however, once again run into the problem of gauge fixing as we did in the previous attempt. However, the gauge freedom here is of a different nature, and we are able to provide a procedure for fixing the gauge.

6.2.1 Gauge freedom in tensor networks

The gauge freedom we are dealing it with here is actually a feature of any tensor network. It arises from the fact that the insertion of the identity on any contracted leg will obviously leave the network unchanged. However, if this identity is then decomposed into some matrix X and it's inverse X^{-1} we can then absorb these two factors into the definition of tensors attached to the leg.

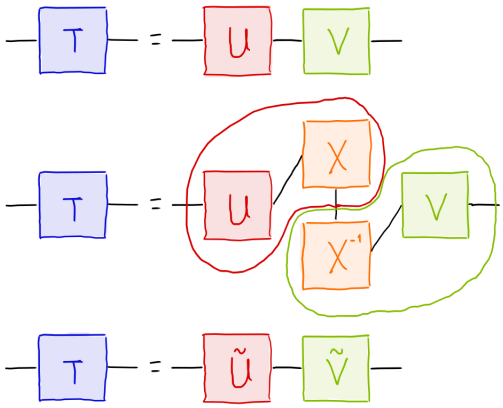

Figure 19: Here we have the graphical representation of the gauge freedom demonstrated in Eq. (121)

This can be illustrated with the following simple example,

$$\begin{aligned} T^a_b &= U^a_c V^c_b, \\ &= U^a_c \delta^c_d V^d_b, \\ &= U^a_c X^c_e (X^{-1})^e_d V^d_b, \\ &= \tilde{U}^a_e \tilde{V}^e_b, \end{aligned} \tag{121}$$

where in the last line we define $\tilde{U}^a_e = U^a_c X^c_e$ and $\tilde{V}^e_b = (X^{-1})^e_d V^d_b$. This procedure is also outlined in the graphical representation in Fig. 19. The output of this small tensor network is then unchanged for such a transformation. Since this is valid for any invertable matrix X, and in larger tensor networks a similar transformation can be applied to every contracted leg, there is clearly a large amount of gauge freedom in all tensor networks. If then, we want to somehow interpret the bulk dynamics as being encoded in the way the tensors evolve in time we had better find a way to fix this gauge freedom. We will now present two methods to do so for MERA networks.

6.2.2 Gauge fixing MERA

To begin our gauge fixing procedure we need to introduce the *bond density matrix*, to do this it will useful to consider the sequence states defined by a MERA, where the states in the sequence correspond to applying more and more layers of isometris and disentanglers to the top tensor, i.e. for MERA network

$\mathcal{M}$ we obtain

$$\begin{aligned}
&\mathcal{M} \to \{|\psi_0\rangle, |\psi_1\rangle, |\psi_2\rangle, |\psi_3\rangle \dots\}, \\
&|\psi_1\rangle = W_1 |\psi_0\rangle, \\
&|\psi_2\rangle = U_1 |\psi_1\rangle, \\
&|\psi_3\rangle = W_2 |\psi_2\rangle, \\
&\text{etc.}
\end{aligned}$$

where $|\psi_0\rangle$ corresponds to the top tensor and W_i is the tensor defined by the tensor product of all isometies in the ith layer, and similarly for U_i and the disentanglers. With this in hand we can now define the bond density matrix.

Definition 7. *For a some contracted leg, l, in a MERA network, $\mathcal{M}$, there is a unique state, $|\psi\rangle$, in the sequence of states defined by $\mathcal{M}$ such that l is free. We then define the bond density matrix of leg l as,*

$$\rho_l = \mathrm{Tr}_{\bar{l}} \left[|\psi\rangle \langle\psi| \right],$$

where we have taken the partial trace over all other legs in $|\psi\rangle$.

From here we have two options for how to fix the gauge. The first we will present has the advantage of maintaining the unitarity of the individual tensors in the network. Since this quality is essential for the efficient calculation of expectation values this is obviously desirable. However, this choice doesn't really tell us anything about the emergent geometry. The second choice however, will break unitarity but will allow for a more precise interpretation of the bulk geomtry than we have seen so far.

Diagonal gauge The diagonal gauge is defined as the gauge choice in which the bond density matrix on every leg is diagonalized. We start then by obtaining the bond density matrix for a leg as described in Def. 7, and then eigendecompose the matrix,

$$\begin{aligned}
\rho_l &= \mathrm{Tr}_{\bar{l}} \left[|\psi\rangle \langle\psi| \right] \\
&= u_l D_l u_l^\dagger,
\end{aligned} \tag{122}$$

from which it is straight forward to diagonalize,

$$D_l = \mathrm{Tr}_{\bar{l}} \left[(u_1^\dagger \otimes I_{\bar{l}}) |\psi\rangle \langle\psi| (u_1 \otimes I_{\bar{l}}) \right]. \tag{123}$$

So we see that to diagonalize the bond density matrix we must absorb $u_l^\dagger$ into the tensor attached to the leg on end the towards the centre of the network, and then to prevent changing the state on the boundary we must also absorb u_l into the tensor attached to the leg on the boundary pointing end. Apply this same process to every contracted leg in the network we will have then entirely fixed the gauge freedom. However as we mentioned this has not provided us with any new insights into the holographic properties of the network, other than what has already been established in section 5. We turn now then to the other option.

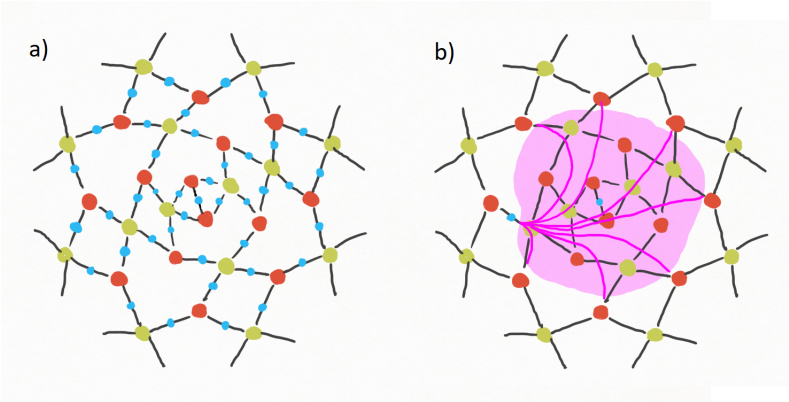

Figure 20: a) A periodic MERA network with the centreless gauge applied, where the blue circles are the bond matrices. b) The isometric flow has been visualized for a particular bond matrix. The pink region is globally an isometry from the shown bond matrix to the other legs at the same depth. The pink lines then indicate the flow

Centreless gauge The centreless gauge follows directly from the diagonal gauge. However, in applying this gauge we will not only alter the tensors themselves but also change the structure of the network itself. We begin with a MERA network, $\mathcal{M}$, that has already been put in the diagonal gauge, where the sequence of states are now such that all 1-site density matrices are diagonal. We then start by selecting a leg l, for which we also have the state, $|\psi\rangle$, from the sequence, which is the state such that l is an open leg. We then Schmidt decompose $|\psi\rangle$ between l and $\bar{l}$,

$$|\psi\rangle = \sum_i s_i \, |i\rangle_l \, |e_i\rangle_{\bar{l}} \,, \tag{124}$$

where we see that l is indeed diagonalized, and the $|e_i\rangle$ are orthonormal. Note that in applying the diagonal gauge we already obtained the singular values s_i since they are simply the square root of the eignvalues of ρ_l. We now define S_l as the diagonal matrix of singular values, ($S_l^2 = D_l$). If the inverse of this matrix is then applied to the state we will obtain an unnormalized maximally entangled state,

$$(S_l^{-1} \otimes I_{\bar{l}}) \, |\psi\rangle = \sum_i |i\rangle_l \, |e_i\rangle_{\bar{l}} \,. \tag{125}$$

However, we know that under the Choi-Jamiołkowski isomorphism this is equivalent to an isometry from l to $\bar{l}$

$$V_\psi = \sum_i |e_i\rangle_{\bar{l}} \, \langle i|_l \,. \tag{126}$$

We will return to this point in a moment as first we obviously need to insert a factor of S_l so that the output of the network is not effected. However this

time, instead of absorbing it into the definition of the other tensor on the leg we will simply leave it on the leg as a *bond matrix*. We now also note that this bond matrix is a quantum state under the Choi-Jamiołkowski isomorphism,

$$\begin{aligned} S_l &= \sum_i s_i \left|i\right\rangle \left\langle i\right| , \\ \left|S_l\right\rangle &= \sum_i s_i \left|i\right\rangle \left|i\right\rangle . \end{aligned} \tag{127}$$

We see now why this is the *centreless* gauge, since after we apply this same process to every contracted leg *except* those attached to the top tensor, we will have a top tensor like state on every leg, and further still as a consequence of the fact that,

$$(I \otimes V_\psi \left|S_l\right\rangle) = \left|\psi\right\rangle , \tag{128}$$

the global isometric property of the network can be shown to flow away from any bond matrix to the boundary, no long exclusively the top tensor. It is important to note that none of the individual tensors will be isometric as we have absorbed non-unitary matrices into their definition. It is only the entire subnetwork that defines V_ψ that acts isometrically from l to $\bar{l}$, and similarly for each other leg in the network. A graphical representation of a MERA network in the centreless gauge as well as a visualization of the isometric flow can be seen in Fig. 20. The procedure here can be seen as a special case of the more general method of gauge fixing networks with closed loops provided in [71].

6.2.3 Emergent geometry in the centreless gauge

We mentioned that at the cost of breaking unitarity in the centreless gauge we would obtain a better understanding of the emergent bulk geometry. We now turn our attention to this property.

As a consequence of the fact that we have extracted the singular values of each bond onto the leg itself, we can now easily associate an entropy with each leg in the network. Since $S_l^2 = D_l$, and D_l is simply the eigenvalues of the bond density matrix, the entropy of the bond density matrix is as follows,

$$S(\rho_l) = \mathrm{Tr}\big[-S_l^2 \log\big(S_l^2\big)\big]. \tag{129}$$

Similar to how in section 5 we provided an upper bound on the entropy of a bulk curve and then equated this to the length of the curve we can now provide a similar but tighter bound on the entropy of a curve in the centreless gauge. Namely for a bulk curve γ we have, as a consequence of subadditivity,

$$S(\gamma) \leq \sum_{l \in \gamma} S_l \tag{130}$$

where we are summing over all the legs that γ intersects, S_l here is a short hand for $S(\rho_l)$. First, we not that this is clearly a tighter bound as our previous bound was just the maximum possible entropy. Second, this bound is actually

state dependent where as the original was just a consequence of the network structure. Finally we note the structural similarity between this equation and the equation for curve length in relativity,

$$\sum_{l\in\gamma} S_l \approx \int_\gamma ds. \tag{131}$$

We can then postulate that the bond matrices in the centreless gauge approximately define a metric like structure on the bulk that will change as we time evolve the boundary state. We then propose the following method for extracting bulk dynamics.

- For some critical Hamiltonian of the boundary system we apply the usual variational algorithm [63] to obtain the ground state.
- We then perturb the system by changing one of the tensors in the network to some other isometry or unitary.
- We apply the centreless gauge to the resulting network and record the bond entropies.
- Using the algorithm of [69] we then time evolve the boundary state.
- At each time increment we again apply the centreless gauge and record bond entropies.

The hope then is that from the data generated by this method, we can determine some behaviour that is reminisent of how the induced metric on a sequence of timeslices that foliate an AdS spacetime would evolve.

7 Conclusion

In this thesis, we have studied the prospects of using holographic tensor networks as models for bulk dynamics. We explored the strengths and weaknesses of both MERA and HaPPY networks in achieving this goal. We found that MERA networks have the advantage of having an associated Hamiltonian, allowing for the simulation of time evolution. However, holographic properties are only approximately satisfied. Counter to this, HaPPY networks exhibit many holographic properties exactly, but unfortunately are not associated with any physical system and so cannot be assigned a Hamiltonian. The goal then was to find a middle ground between these two methods.

We presented two possible approaches. The first is based on a MERA network that has been modified such that it describes a unitary map between the bulk and boundary Hilbert spaces. Using this map a bulk Hamiltonian can then be obtained from the Hamiltonian of the boundary. However, we ran into issues with this attempt as the tensors in the network that posses the bulk legs are underconstrained. This prevented us from obtaining a unique bulk Hamiltonian.

In future work it may be possible to find a sensible constraint such that the bulk Hamiltonian is unique. A potential approach to constrain these tensors is to choose them such that bulk non-locality is maximally suppressed, but the manner in which this can be achieved is unclear.

In the second approach we again use the MERA network, not as a bulk to boundary map, but in its original form as an ansatz. In this approach we aimed to interpret the the bulk dynamics in terms of how the tensors themselves evolve. We again ran into a problem of the tensors being underconstrained. This was manifestation of a property inherent to all tensor networks in which there is a gauge freedom for every contracted leg in the network. However, we were able to provide a method of fixing this gauge freedom such that the bulk geometry is more manifest. In this centreless gauge a bond matrix is associated to every contracted leg, and from these bond matrices an entropy can be obtained, which the Ryu-Takayanagi proposal tells us is dual to a bulk area, or length in the case of 1+1D boundary. The bond matrices then seem then to provide a metric like structure in the bulk. We then propose a method that combines the centreless gauge with the algorithms of [63] and [69] to record how this metric like structure evolves in time.

There are some interesting open question in this centreless gauge approach. First, how should we interpret the tensors in the network other than the bond matrices? In the original MERA these are the isometries and disentanglers, but our gauge-fixing approach breaks the isometric property of these tensors. It is a certainty that there is more information about the bulk geometry to be gleaned from these tensors since the single leg entropies defined by the bond matrices provide a far from a complete picture of the entanglement structure. However how to extract this information is unclear. It is also a possibility that the bulk fields are encoded in these tensors but it is unclear if this notion can be made precise. Another interesting question is, in what manner and to what degree do the bond matrices provide a metric like structure? Generating some numerical data with the method described will likely shed some light on this question, and perhaps provide some insight into how the association can be made precise.

Acknowledgements

I would first of all like to thank my advisor, Wilke van der Schee, whose guidance through the vast range of prerequisite topics necessary for this research, I would have been lost without. Second, I would like to thank my friends and family. The moral support that they have provided me over the last year has been essential in getting over the finish line, and without it I feel I would not have overcome the various periods of difficulty I have encountered in my work. In particular I would like to thank those who were brave enough to indulge me in talking about my research. These conversations often led me to think more deeply about aspects I had previously overlooked and at times led to some surprisingly pertinent questions. Last but certainly not least, I would like to give special thanks to my parents who have financially supported me throughout my degree. I am eternally grateful for the opportunities they have provided me with.

References

[1] John F. Donoghue. "General relativity as an effective field theory: The leading quantum corrections". In: *Phys. Rev. D* 50 (6 1994). DOI: 10.1103/PhysRevD.50.3874.

[2] G. 't Hooft. *Dimensional Reduction in Quantum Gravity*. 2009. arXiv: gr-qc/9310026 [gr-qc].

[3] Leonard Susskind. "The world as a hologram". In: *Journal of Mathematical Physics* 36.11 (1995). ISSN: 0022-2488. DOI: 10.1063/1.531249.

[4] Jacob D. Bekenstein. "Black Holes and Entropy". In: *Phys. Rev. D* 7 (8 1973). DOI: 10.1103/PhysRevD.7.2333.

[5] Juan Maldacena. In: *International Journal of Theoretical Physics* 38.4 (1999). DOI: 10.1023/A:1026654312961.

[6] Subir Sachdev. "Condensed Matter and AdS/CFT". In: *Lecture Notes in Physics*. Springer Berlin Heidelberg, 2011. ISBN: 9783642048647. DOI: 10.1007/978-3-642-04864-7_9.

[7] Ofer Aharony. *The non-AdS/non-CFT correspondence, or three different paths to QCD*. 2003. arXiv: hep-th/0212193 [hep-th].

[8] Bowen Chen, Bartłomiej Czech, and Zi-Zhi Wang. "Quantum information in holographic duality". In: *Reports on Progress in Physics* 85.4 (2022). DOI: 10.1088/1361-6633/ac51b5.

[9] Shinsei Ryu and Tadashi Takayanagi. "Aspects of holographic entanglement entropy". In: *Journal of High Energy Physics* 2006.08 (2006).

[10] A. Almheiri and D. Harlow. "Bulk locality and quantum error correction in AdS/CFT". In: *JHEP* 2015:163 (2015).

[11] Brian Swingle. "Entanglement renormalization and holography". In: *Phys. Rev. D* 86 (6 2012). DOI: 10.1103/PhysRevD.86.065007.

[12] F. Pastawski et al. "Holographic quantum error-correcting codes: toy models for the bulk/boundary correspondence". In: *JHEP* 2015:149 (2015).

[13] Román Orús. "Tensor networks for complex quantum systems". In: *Nature Reviews Physics* 1.9 (2019). DOI: 10.1038/s42254-019-0086-7.

[14] G. Vidal. "Entanglement Renormalization". In: *Phys. Rev. Lett.* 99 (22 2007). DOI: 10.1103/PhysRevLett.99.220405.

[15] Patrick Hayden et al. "Holographic duality from random tensor networks". In: *Journal of High Energy Physics* 2016.11 (2016). DOI: 10.1007/jhep11(2016)009.

[16] Pawel Caputa, Jorrit Kruthoff, and Onkar Parrikar. "Building tensor networks for holographic states". In: *Journal of High Energy Physics* 2021.5 (2021). DOI: 10.1007/jhep05(2021)009.

[17] Ning Bao et al. "Beyond toy models: distilling tensor networks in full AdS/CFT". In: *Journal of High Energy Physics* 2019.11 (2019). DOI: 10.1007/jhep11(2019)069.

[18] Masamichi Miyaji and Tadashi Takayanagi. "Surface/state correspondence as a generalized holography". In: *Progress of Theoretical and Experimental Physics* 2015.7 (2015). DOI: 10.1093/ptep/ptv089.

[19] Koji Umemoto and Tadashi Takayanagi. "Entanglement of purification through holographic duality". In: *Nature Physics* 14.6 (2018). DOI: 10.1038/s41567-018-0075-2.

[20] Victor Chua et al. "Holographic dynamics from multiscale entanglement renormalization ansatz". In: *Phys. Rev. B* 95 (19 2017). DOI: 10.1103/PhysRevB.95.195152.

[21] A. May. "Tensor networks for dynamic spacetimes". In: *Journal of High Energy Physics* 2017.6 (2017). DOI: 10.1007/jhep06(2017)118.

[22] Tobias J. Osborne and Deniz E. Stiegemann. "Dynamics for holographic codes". In: *Journal of High Energy Physics* 2020.4 (2020). DOI: 10.1007/jhep04(2020)154.

[23] Matheus H. Martins Costa et al. "Wilsonian renormalization as a quantum channel and the separability of fixed points". In: *Phys. Rev. D* 107 (12 2023). DOI: 10.1103/PhysRevD.107.125014.

[24] Pragati Gupta and C. M. Chandrashekar. "Optimal quantum simulation of open quantum systems". In: (2020). arXiv: 2012.07540 [quant-ph].

[25] Man-Duen Choi. "Completely positive linear maps on complex matrices". In: *Linear Algebra and its Applications* 10 (1975). DOI: 10.1016/0024-3795(75)90075-0.

[26] A. Jamiołkowski. "Linear transformations which preserve trace and positive semidefiniteness of operators". In: *Reports on Mathematical Physics* 3 (1972). DOI: 10.1016/0034-4877(72)90011-0.

[27] C. E. Shannon. "A mathematical theory of communication". In: *The Bell System Technical Journal* 27 (1948). DOI: 10.1002/j.1538-7305.1948.tb01338.x.

[28] H. Araki and E.H. Lieb. "Entropy inequalities". In: *Commun.Math. Phys.* 18 (1970). DOI: 10.1007/BF01646092.

[29] Elliott H. Lieb and Mary Beth Ruskai. "Proof of the strong subadditivity of quantum-mechanical entropy". In: *Journal of Mathematical Physics* 14.12 (1973). DOI: 10.1063/1.1666274.

[30] A. Einstein, B. Podolsky, and N. Rosen. "Can Quantum-Mechanical Description of Physical Reality Be Considered Complete?" In: *Phys. Rev.* 47 (10 1935). DOI: 10.1103/PhysRev.47.777.

[31] Asher Peres and Daniel R. Terno. "Quantum information and relativity theory". In: *Rev. Mod. Phys.* 76 (1 2004). DOI: 10.1103/RevModPhys.76.93.

[32] Sevag Gharibian. *Strong NP-Hardness of the Quantum Separability Problem*. 2009. arXiv: 0810.4507 [quant-ph].

[33] I. Bengtsson and K. Zyczkowski. *Geometry of Quantum States: An Introduction to Quantum Entanglement*. Cambridge: Cambridge University Press, 2006.

[34] M. Nielsen and I. Chuang. *Quantum Computation and Quantum Information*. Cambridge: Cambridge University Press, 2000.

[35] S. W. Hawking. "Gravitational Radiation from Colliding Black Holes". In: *Phys. Rev. Lett.* 26 (21 1971). DOI: 10.1103/PhysRevLett.26.1344.

[36] S. W. Hawking. "Particle creation by black holes". In: *Commun. Math. Phys.* 43 (3 1975). DOI: 10.1007/BF02345020.

[37] Ahmed Almheiri et al. "The entropy of Hawking radiation". In: *Rev. Mod. Phys.* 93 (3 2021). DOI: 10.1103/RevModPhys.93.035002.

[38] Veronika E Hubeny, Mukund Rangamani, and Tadashi Takayanagi. "A covariant holographic entanglement entropy proposal". In: *Journal of High Energy Physics* 2007.07 (2007). DOI: 10.1088/1126-6708/2007/07/062.

[39] Thomas Faulkner, Aitor Lewkowycz, and Juan Maldacena. "Quantum corrections to holographic entanglement entropy". In: *Journal of High Energy Physics* 2013.11 (2013). DOI: 10.1007/jhep11(2013)074.

[40] Netta Engelhardt and Aron C. Wall. "Quantum extremal surfaces: holographic entanglement entropy beyond the classical regime". In: *Journal of High Energy Physics* 2015.1 (2015). DOI: 10.1007/jhep01(2015)073.

[41] Stephen A. Fulling. "Nonuniqueness of Canonical Field Quantization in Riemannian Space-Time". In: *Phys. Rev. D* 7 (10 1973). DOI: 10.1103/PhysRevD.7.2850.

[42] P C W Davies. "Scalar production in Schwarzschild and Rindler metrics". In: *Journal of Physics A: Mathematical and General* 8.4 (1975). DOI: 10.1088/0305-4470/8/4/022.

[43] W. G. Unruh. "Notes on black-hole evaporation". In: *Phys. Rev. D* 14 (4 1976). DOI: 10.1103/PhysRevD.14.870.

[44] Richard C. Tolman. "On the Weight of Heat and Thermal Equilibrium in General Relativity". In: *Phys. Rev.* 35 (8 1930). DOI: 10.1103/PhysRev.35.904.

[45] D. Harlow. "Jerusalem lectures on black holes and quantum information". In: *Rev. Mod. Phys.* 88 (1 2016). DOI: 10.1103/RevModPhys.88.015002.

[46] Daniel Harlow and Douglas Stanford. *Operator Dictionaries and Wave Functions in AdS/CFT and dS/CFT*. 2011. arXiv: 1104.2621 [hep-th].

[47] Mukund Rangamani and Tadashi Takayanagi. *Holographic Entanglement Entropy*. Springer International Publishing, 2017. ISBN: 9783319525730. DOI: 10.1007/978-3-319-52573-0.

[48] Juan Maldacena. "Eternal black holes in anti-de Sitter". In: *Journal of High Energy Physics* 2003.04 (2003). DOI: 10.1088/1126-6708/2003/04/021.

[49] M. Van Raamsdonk. "Building up spacetime with quantum entanglement". In: *Gen Relativ Gravit* 42 (2010). DOI: 10.1007/s10714-010-1034-0.

[50] Aron C Wall. "Maximin surfaces, and the strong subadditivity of the covariant holographic entanglement entropy". In: *Classical and Quantum Gravity* 31.22 (2014). DOI: 10.1088/0264-9381/31/22/225007.

[51] Bartłomiej Czech et al. "The gravity dual of a density matrix". In: *Classical and Quantum Gravity* 29.15 (2012). DOI: 10.1088/0264-9381/29/15/155009.

[52] Matthew Headrick et al. "Causality and holographic entanglement entropy". In: *Journal of High Energy Physics* 2014.12 (2014). DOI: 10.1007/jhep12(2014)162.

[53] Daniel L. Jafferis et al. "Relative entropy equals bulk relative entropy". In: *Journal of High Energy Physics* 2016.6 (2016). DOI: 10.1007/jhep06(2016)004.

[54] Xi Dong, Daniel Harlow, and Aron C. Wall. "Reconstruction of Bulk Operators within the Entanglement Wedge in Gauge-Gravity Duality". In: *Physical Review Letters* 117.2 (2016). DOI: 10.1103/physrevlett.117.021601.

[55] Geoffrey Penington. *Entanglement Wedge Reconstruction and the Information Paradox*. 2020. arXiv: 1905.08255 [hep-th].

[56] Steven R. White. "Density matrix formulation for quantum renormalization groups". In: *Phys. Rev. Lett.* 69 (19 1992). DOI: 10.1103/PhysRevLett.69.2863.

[57] L. Tagliacozzo and G. Vidal. "Entanglement renormalization and gauge symmetry". In: *Phys. Rev. B* 83 (11 2011). DOI: 10.1103/PhysRevB.83.115127.

[58] Szilárd Szalay et al. "Tensor product methods and entanglement optimization for ab initio quantum chemistry". In: *International Journal of Quantum Chemistry* 115.19 (2015). DOI: 10.1002/qua.24898.

[59] Yoav Levine et al. "Quantum Entanglement in Deep Learning Architectures". In: *Physical Review Letters* 122.6 (2019). DOI: 10.1103/physrevlett.122.065301.

[60] M B Hastings. "An area law for one-dimensional quantum systems". In: *Journal of Statistical Mechanics: Theory and Experiment* 2007.08 (2007). DOI: 10.1088/1742-5468/2007/08/P08024.

[61] Leo P. Kadanoff. "Scaling laws for ising models near T_c". In: *Physics Physique Fizika* 2 (6 1966). DOI: 10.1103/PhysicsPhysiqueFizika.2.263.

[62] Markus Hauru, Maarten Van Damme, and Jutho Haegeman. "Riemannian optimization of isometric tensor networks". In: *SciPost Phys.* 10 (2021). DOI: 10.21468/SciPostPhys.10.2.040.

[63] G. Evenbly and G. Vidal. "Algorithms for entanglement renormalization". In: *Phys. Rev. B* 79 (14 2009). DOI: 10.1103/PhysRevB.79.144108.

[64] Charles H. Bennett et al. "Teleporting an unknown quantum state via dual classical and Einstein-Podolsky-Rosen channels". In: *Phys. Rev. Lett.* 70 (13 1993). DOI: 10.1103/PhysRevLett.70.1895.

[65] Wolfram Helwig et al. "Absolute maximal entanglement and quantum secret sharing". In: *Phys. Rev. A* 86 (5 2012). DOI: 10.1103/PhysRevA.86.052335.

[66] D. Harlow. "The Ryu–Takayanagi Formula from Quantum Error Correction". In: *Commun. Math. Phys* 2017:354 (2017).

[67] X. Dong. "The gravity dual of Rényi entropy". In: *Nature Commun.* 7 (2016). DOI: 10.1038/ncomms12472.

[68] Guifré Vidal. "Efficient Classical Simulation of Slightly Entangled Quantum Computations". In: *Phys. Rev. Lett.* 91 (14 2003). DOI: 10.1103/PhysRevLett.91.147902.

[69] Matteo Rizzi, Simone Montangero, and Guifre Vidal. "Simulation of time evolution with multiscale entanglement renormalization ansatz". In: *Phys. Rev. A* 77 (5 2008). DOI: 10.1103/PhysRevA.77.052328.

[70] X. Dong, D. Harlow, and D. Marloff. "Flat entanglement spectra in fixed-area states of quantum gravity". In: *JHEP* 240 (2019). DOI: 10.1007/JHEP10(2019)240.

[71] Glen Evenbly. "Gauge fixing, canonical forms, and optimal truncations in tensor networks with closed loops". In: *Phys. Rev. B* 98 (8 2018). DOI: 10.1103/PhysRevB.98.085155.